

# Excitonic Coupled-cluster Theory

Yuhong Liu, Anthony D. Dutoi\*

*Department of Chemistry, University of the Pacific, Stockton, California 95211, USA*

\*adutoi@pacific.edu

December 8, 2022

## Abstract

A generalized variant of coupled-cluster theory is described here, wherein the degrees of freedom are fluctuations of fragments between internally correlated states. The effects of intra-fragment correlation on the inter-fragment interaction are pre-computed and permanently folded into an effective Hamiltonian, thus avoiding many redundant evaluations of local relaxations associated with coupled fluctuations. A companion article shows that the electronic Hamiltonians of real systems may always be cast in the form required. Two proof-of-principle demonstrations are presented. One uses harmonic oscillators, for which accuracy and algorithm structure can be carefully controlled in comparisons. The other uses small electronic systems to demonstrate compelling accuracy and efficiency, also when inter-fragment electron exchange and charge transfer must be handled. This framework opens a promising path to build finely tunable, systematically improvable methods to capture precise properties of systems interacting with a large number of other systems. Since this scheme is independent of the quality of the states used for the fragments, it can be arbitrarily detailed in terms of the correlation model used for each. The extension to excited states is also straightforward.

# 1 Introduction

Starting a few decades ago, and continuing apace today, enormous progress is being made in performing useful chemical simulations by decomposing large quantum-mechanical systems into recoupled sub-systems. The state of the art generally consists of embedding fragments into the electrostatic environments of their neighbors (with various approaches to the exchange interaction),<sup>1–9</sup> or using a fragment-based decomposition of a reference wavefunction for electron-correlation calculations;<sup>10,11</sup> these approaches may be taken in combination with schemes for configurational sampling and techniques for handling redundancy in periodic systems.<sup>12–14</sup> The literature chronicling the evolution of fragment-based methods is vast, and has been reviewed several times.<sup>15–18</sup>

Notwithstanding all of this progress, a more favorable ratio of accuracy to computational cost is always desirable, in order to broaden the coverage of reliable simulations, especially if the phenomena under investigation hinge on small energy differences or require a level of electronic detail not afforded by presently applicable wavefunctions or density functionals. There exists a present need for an *ab initio* scheme of recoupling fragments, which has both a well-defined progression towards exactness and a flexible scheme of approximations. Systematic improvability is the only way to rigorously demonstrate the reliability of a model in the context of a *specific* problem.

This article describes and tests a generalized variant of the coupled-cluster (CC) model. The CC wavefunction is quite general with respect to the degrees of freedom to which it can be applied (see, for example, vibrational CC<sup>19–21</sup>), and the operative paradigm in this work is to use state-to-state fluctuations of entire fragments, rather than individual particle or inter-particle coordinates. The method is called excitonic CC (X-CC), since such fluctuations form the conceptual site basis from which Frenkel–Davydov excitons<sup>22–26</sup> are built. The potential power of this approach is rooted in restricting each fragment to the space of its lowest-energy *internally correlated* states, thus compressing the description of the most relevant part of the Hilbert space.

In a companion article, the electronic Hamiltonian for a general chemical system was decomposed by fragments, in precisely the manner necessary to apply the X-CC model. Charge-transfer and inter-fragment electron exchange were handled rigorously, and it was shown that systematically improvable approximate Hamiltonians can be tractably constructed, by admit-

ting a variable number of many-electron states for each fragment. Though the use of high-quality states for the fragments will impact the computational cost of constructing an effective Hamiltonian (scaling only quadratically with system size, however), the cost of the X-CC method described herein depends only on the number of states per fragment. The level of approximation may be finely tuned by the choice of both the electronic structure method for the fragments (possibly different for each fragment) and the number of states admitted for each fragment. Since the method can be made exact, systematic studies of sources of error can be made, thus aiding in the development of judicious approximations.

To elucidate the potential of the proposed paradigm mechanistically, consider that the usual description of dispersion forces requires at least a connected double substitution, already exhausting the excitation level that is available in conventional CC theory with single and double substitutions (CCSD). Corrections to fragment polarizabilities, due to local electronic relaxations, will show up first when higher substitutions are included, such as with full or perturbative inclusion of connected triples [CCSDT or CCSD(T), respectively], the present “gold standards” of quantum chemistry. In contrast, if up to connected double substitutions of primitive electrons were to enter the *fragment* wavefunctions of an overall X-CC wavefunction with up to connected *dimer* fluctuations (X-CCSD), this would automatically include implicit contributions from primitive connected quadruple substitutions. For these reasons, it is not unreasonable to suggest that a practicable method might be built that can exceed the accuracy of a hypothetical conventional CCSDT calculation for systems that are well out of reach for even conventional CCSD.

Another perspective on the justification for treating intra- and inter-fragment correlation on different footings is that the effective interactions between fragments decay much faster than the bare Coulomb potential. Fluctuations of fragments are described well as being a small perturbation away from independent of one another, whereas fluctuations of individual electrons within a fragment are highly entangled. These internal correlations, and the associated electronic relaxations accompanying local charge fluctuations, are computed once per fragment and permanently folded into the Hamiltonian.

Fragment states and fragment-decomposed Hamiltonians have a long and continuing history in quantum chemistry. Symmetry-adapted perturbation theory (SAPT)<sup>10</sup> is rooted in the early work of of London, Axilrod, and Teller, among others, which begins by expressing intermolec-

ular interactions as sums over fragment eigenstates.<sup>27</sup> The SAPT(CC) approach, in particular, handles intra-fragment correlation by applying a CC transformation to the fragment states.<sup>28</sup> Enforcing global antisymmetry for general systems in SAPT is unwieldy, however, and only rare applications beyond dimers are found.<sup>29</sup> The recently proposed molecular cluster perturbation theory<sup>11</sup> also divides the super-system Hamiltonian into fragment terms and interactions, but global antisymmetry is neglected.

In low-order perturbative approaches, in general, it is unnecessary to transform the many-electron bases of the fragments, since this can be incorporated into the non-iterative action of the Hamiltonian at no additional cost. The motivations for proceeding beyond low-order perturbation theory are manifold, however. To begin with, long-range induction and other cooperative effects can be substantial and occur at relatively high orders of perturbation theory (*e.g.*, 4th).<sup>30,31</sup> In addition to this, one expects further errors if polarizabilities from mean-field descriptions of the fragments are used; excitation energies control the “stiffness” of a charge distribution (perturbative denominators), and these are known to be quite sensitive to correlation level.<sup>32</sup> There is also dynamical screening or cooperation between fluctuations, collectively known as many-body dispersion (a “body” is a fragment), which are missing at low orders of perturbation theory, and this has been shown to be important.<sup>29,33</sup>

Choosing the many-electron basis for each fragment will clearly play a decisive role in the efficiency of an actual X-CC calculation. It is important then to mention the success of the density matrix renormalization group (DMRG) in iteratively developing optimal reduced subsystem bases for tensor-network states.<sup>34–36</sup> While this aspect is similar in spirit to X-CC, the global wavefunction is very different in structure. We might anticipate lesser success with X-CC when near neighbors are highly entangled; however, a more efficient treatment of system-wide dynamical correlation (a known weakness of DMRG) should result from the exponential Ansatz, which cleanly separates connected (correlated) and disconnected (coincidental) simultaneous fluctuations. The X-CC approach also does not exclude iterative optimization of the fragment bases.

In this article, we provide the essential equations describing the X-CC model. Two methodological tests are undertaken. In one case, the super-system is composed of model “molecules” that are internally constructed of coupled harmonic oscillators. The ease of implementation and availability of the exact solution for that problem allow for rigorous comparisons of errors

and computational cost for similarly structured primitive and excitonic algorithms. To provide initial evidence that the promising results apply also to electronic systems, accounting for inter-fragment electron exchange and charge transfer, X-CC is applied to chains of up to 100 Be atoms.

## 2 Theory

Following the notation established in the companion article, a subscript on an index  $i_m$  of a many-electron state serves to restrict that index to those values associated with a given fragment  $m$ . Lower-case latin letters are used for integer indices, and upper-case latin letters are used for indices that are ascending-ordered tuples of integers, for example,  $I = (i_1, \dots, i_{\ell_I})$ . The indexing of the elements of tuple  $I$  as  $i_m$  will always coincide here with our notation for restricting those indices to specific fragments, conveniently avoiding ambiguity. Sets are denoted as  $\{y_i\}$ , containing members  $y_i$  for all values of  $i$  allowed by a mapping  $y$ . A summation over an index implicitly runs over all values allowed by the mapping to which that index is attached.

### 2.1 Fluctuation Operators

Consider a generic super-system composed of  $N$  fragments. Given a complete basis  $\{|\psi_{i_m}\rangle\}$  for the many-body state space of each fragment  $m$ , we start with the assumption that the super-system state space is completely spanned by a set of states  $\{|\Psi_I\rangle\}$ , each having the form

$$|\Psi_I\rangle = |\psi_{i_1} \dots \psi_{i_N}\rangle \quad (1)$$

with  $I = (i_1, \dots, i_N)$ . This notation is intended to imply, foremostly, that  $|\Psi_I\rangle$  is tensor-product-like in structure, such that it is meaningful to say that fragment  $m$  is in state  $|\psi_{i_m}\rangle$ . By collecting the fragment-state labels into a single ket, it is implied that this is also a valid state for the overall system, having proper inter-particle exchange symmetry among the primitive coordinates (*e.g.*, electrons).

We next assert the existence of a set of fluctuation operators  $\{\hat{\tau}_i^j\}$ , where the lower and upper indices of each operator identify two states  $|\psi_i\rangle$  and  $|\psi_j\rangle$  (possibly the same), which must belong to the same fragment. The action of  $\hat{\tau}_{i_m}^{j_m}$  onto basis state  $|\Psi_K\rangle$  is defined as

changing the state of fragment  $m$  according to

$$\hat{\tau}_{i_m}^{j_m} |\psi_{k_1} \cdots \psi_{k_m} \cdots \psi_{k_N}\rangle = \delta_{j_m, k_m} |\psi_{k_1} \cdots \psi_{i_m} \cdots \psi_{k_N}\rangle \quad (2)$$

This action is constructed to be reminiscent of a number-conserving pair of field operators onto a single-determinant electronic state, such that the null state results if the upper (“destruction”) index corresponds to an “empty” fragment state. These operators have the following commutation relation by construction

$$[\hat{\tau}_i^j, \hat{\tau}_k^l] = \delta_{jk} \hat{\tau}_i^l - \delta_{il} \hat{\tau}_k^j \quad (3)$$

This is shown from the definition in eq. (2) by noting, first, that operators on different fragments commute, and, second, that a string of two operators on the same fragment gives null if the upper index of the left operator does not match the lower index of the right operator. (The preference for positioning indices is clarified in the companion article.)

The assumptions that (1) a set of tensor products of fragment states builds a complete basis for the super-system space and that (2) the asserted fluctuation operators are well-defined in that space are points that need to be proven for different classes of systems. For the oscillator-model fragments explored in this work (closed systems with distinguishable coordinates), these assumptions are trivially valid. The effort to show this for fragment-decomposed electronic systems is found in the companion article.

## 2.2 Coupled-cluster Ansatz

According to the forgoing definition of the fluctuation operators, any basis state  $|\Psi_I\rangle$  may be reached from any other basis state  $|\Psi_J\rangle$  via a string of  $N$  (or fewer) fluctuation operators. Combined with the assumption of completeness of this basis, it is then straightforward to show that an arbitrary super-system state has a unique resolution in terms of the full  $N$ th-order CC (FCC) Ansatz applied to a reference state  $|\Psi_O\rangle$  conforming to  $\langle \Psi_{\text{FCC}} | \Psi_O \rangle \neq 0$ , as

$$|\Psi_{\text{FCC}}\rangle = e^{\hat{T}} |\Psi_O\rangle \quad (4)$$

We have hereby identified the tuple  $O = (o_1, \dots, o_N)$  as special, in that  $|\psi_{o_m}\rangle$  is taken to be the reference state of fragment  $m$ . The operator  $\hat{T}$  consists only of fluctuations away from the reference, denoted  $\hat{\tau}_{i_m}^{o_m}$  with  $i_m \neq o_m$ , referred to specifically as *excitations*

$$\hat{T} = \sum_m \sum_{i_m \neq o_m} t^{i_m} \hat{\tau}_{i_m}^{o_m} + \sum_{m_1 < m_2} \sum_{\substack{i_{m_1} \neq o_{m_1} \\ i_{m_2} \neq o_{m_2}}} t^{i_{m_1} i_{m_2}} \hat{\tau}_{i_{m_1}}^{o_{m_1}} \hat{\tau}_{i_{m_2}}^{o_{m_2}} + \dots \quad (5)$$

The notation  $m_1 < m_2$  indicates that the summation runs over all unique pairs (*etc.*) of fragments. As with conventional CC theory, excitation operators all clearly commute with one another.

As an approximation, the expansion of  $\hat{T}$  will generally be truncated at finite fragment order, with the terms written explicitly in eq. (5) being those retained in the X-CCSD variant. In this case, single substitutions are associated with monomers, and doubles are associated with dimers, *etc.* An interesting analogue to a self-consistent-field (SCF) calculation, which would capture long-range induction using polarizabilities from correlated levels of theory, would be the use of only single excitations in  $\hat{T}$  (X-CCS, also labeled X-SCF). Models beyond X-SCF introduce entangled fluctuations among internally correlated fragment states, accounting for dispersion forces, *etc.*, in a manner that is both self-consistent and size-consistent. In all cases, the most powerful local correlations have already been resolved with the introduction of the super-system basis, and the reference already includes a large fraction of correlation. In practice, the state spaces of the fragments are intended to be truncated according to schemes that consider the balance of cost against accuracy of the desired property.

## 2.3 Hamiltonian

With a general wavefunction Ansatz available, the central task is to iteratively determine the amplitudes  $t^{i_m}$ ,  $t^{i_{m_1} i_{m_2}}$ , *etc.*, that approximate the ground state of a Hamiltonian  $\hat{\mathcal{H}}$ . More precisely, the residual of the eigenstate condition must lie outside the space of variations. This involves the familiar step of evaluating the action of the similarity-transformed Hamiltonian  $e^{-\hat{T}} \hat{\mathcal{H}} e^{\hat{T}}$  onto the reference  $|\Psi_O\rangle$ , in the context of a well-chosen non-linear optimization algorithm. The amplitude update is related to the projection of the result of this action into the space spanned by excitations from the reference, up to the specified Ansatz order. Technically, convergence is met when this projection is suitably small, though this is often signaled by the

energy becoming approximately stationary between iterations.

This brings us now to the subject of the Hamiltonian itself. In order to avoid expensive recourse to the primitive degrees of freedom during the amplitude iterations,  $\hat{\mathcal{H}}$  must also be written as an expansion in terms of strings of the fluctuation operators

$$\hat{\mathcal{H}} = \sum_m \sum_{i_m, j_m} H_{j_m}^{i_m} \hat{\tau}_{i_m}^{j_m} + \sum_{m_1 < m_2} \sum_{\substack{i_{m_1}, j_{m_1} \\ i_{m_2}, j_{m_2}}} H_{j_{m_1} j_{m_2}}^{i_{m_1} i_{m_2}} \hat{\tau}_{i_{m_1}}^{j_{m_1}} \hat{\tau}_{i_{m_2}}^{j_{m_2}} + \dots \quad (6)$$

The elements  $H_{j_m}^{i_m}$  build a Hamiltonian matrix for fragment  $m$ , and the higher-order terms are responsible for couplings between fragments (up to  $N$ th order, in principle, depending on the kind of system). If the Hamiltonian is written as such, then a generalized normal ordering of the nested commutators of the Baker–Campbell–Hausdorff (BCH) expansion of  $e^{-\hat{T}} \hat{\mathcal{H}} e^{\hat{T}}$  can be neatly divided into the usual four parts: (1) terms that result in the null state when acting on  $|\Psi_O\rangle$ , (2) a constant, (3) terms representing excitations within the specified Ansatz, and (4) terms representing excitations outside (*e.g.*, higher than) the Ansatz. Part (2) is the pseudo-energy at any iteration, part (3) determines the update to the amplitudes, and parts (1) and (4) need not be computed. The derivation of formulas for these evaluations is discussed in the next section.

At an abstract level it is important to be assured that the BCH expansion does naturally truncate at some low order, so that evaluation of the amplitude updates has manageable computational cost. As in conventional CC theory, if the Hamiltonian itself contains only few-body terms, the requirement for this self-truncation will be fulfilled if the commutator of any two fluctuations is an operator that has both the same excitation rank as the sum of the original two and a fragment rank of less than two.<sup>37</sup> That the fragment rank is reduced by commutation is already manifest in eq. (3). The excitation rank of a string of fluctuations can be defined by subtracting the number of lower indices that refer to a fragment reference state from the number of upper such indices (roughly, number of excitations minus number of de-excitations). In those commutators that are not already zero, these numbers are either individually preserved or each is decremented by one, thus preserving excitation rank. Therefore, the BCH expansion must naturally truncate for this generalized CC model.

We have hereby added a third assertion, that the system Hamiltonian can be written in terms of fragment fluctuations. (The original two concerned basis completeness and existence of the

fluctuation operators.) It is likely possible to prove that these assertions may be fulfilled for broad classes of systems, relying on only benevolent assumptions. However, while interesting, it would be useless without an explicit form and a computational recipe for the scalar coefficients in the expansion of  $\hat{\mathcal{H}}$ . Therefore, we leave these assertions to be validated on a case-by-case basis for each class of systems (*e.g.*, all fragment-decomposed electronic systems). For the oscillator-model fragments in this article, this will be trivial, but, for electronic systems that may overlap and transfer charge, possibly also having linear dependencies in the one-electron basis, the exercise is more intense, and it is undertaken in the companion article.

### 3 Correlation Models and Computation

We now discuss specific models based on the X-CC formalism. The established nomenclature for the CC hierarchy [CCSD, CCSD(T), CCSDT, *etc.*] has already been adopted to reference the included orders of connected simultaneous *fragment* fluctuations. In addition to the correlation level of the wavefunction, there are approximations which may be applied to the excitonic Hamiltonian itself. It is most sensible to include such qualifiers with the prepended excitonic “X.” In this work, we will specifically refer to the methods X2-CCSD and X2-CCSDT, and also to the analogue of full configuration interaction (FCI), X2-FCI. The “2” in this declension indicates that the Hamiltonian contains maximally dimer coupling terms. For electronic systems, this is an approximation because trimer and tetramer terms are missing; these are discussed in the companion article. Other parameters could also be named, in order to also indicate the quality of the fragment states used, *etc.*, but we withhold discussion of this until system details are presented.

A completely in-house implementation of the CC algorithm is used for experimental calculations; evaluation of the BCH expansion is coded in the C programming language and called as a shared library from a generic Python-based quasi-Newton driver, accelerated by direct inversion in the iterative subspace (DIIS).<sup>37</sup> The equations for the BCH evaluation are derived in appendix A, specifically for the X2-CCSD model (up to dimer terms in both  $\hat{\mathcal{H}}$  and  $\hat{T}$ ). Notably, inspection of eq. (26) reveals that the X2-CCSD method formally scales with the third power of the system size for homogeneous systems, and it scales quartically with respect to the number of states per fragment. Although a generalized diagrammatic approach would certainly have

been more elegant (and will be undertaken in the future), these equations are derived here by straightforward algebraic application of the commutator relationship in eq. (3). Some further details concerning two independent implementations of the amplitude equations (one abstract, one efficient), validation of the computer codes, and connections of the amplitude equation to those from conventional electronic CC and vibrational CC are also discussed in appendix A.

The Psi4 1.0.0 package<sup>38</sup> was used to compare both accuracy and timings to conventional CC variants for electronic systems. Psi4 was also used to run FCI benchmark curves. The excitonic Hamiltonians for electronic systems were built using one- and two-electron integrals obtained from the PYQUANTE 1.6.5 package,<sup>39</sup> which consists of easily modified Python modules. All calculations in this work were run on a single 2.6 GHz Intel Xeon (E5) core, with all runtime data kept in 2133 MHz core memory. The X-CC code currently only runs on one thread, and the processor usage of Psi4 was verified during run time. The multicore nodes used were kept free of other computational traffic during timings.

## 4 Proof-of-principle Results

The two kinds of systems explored were chosen to to provide initial evidence that the X-CC formalism holds promise, while offering peculiar ease of implementation and/or special analytical properties. Handling two very different kinds of systems also highlights the level of abstraction at which CC theory is generalized here.

In the first systems, dipole-coupled fragments are groups of internally coupled harmonic oscillators. These systems provide both trivial primitive matrix elements and the opportunity to compare accuracy against an exact solution. The particular ease of implementation of the Hamiltonian allows us to compare X-CC accuracy and timings to an algorithm that operates on primitive oscillator coordinates, but with precisely the same structure and level of optimization. This is intended to mimic a directly comparable conventional CC algorithm, in order to unambiguously expose the advantage of excitonic renormalization of the Hamiltonian.

In the second set of systems, the fragments are beryllium atoms. Although the one-electron basis set is too small to be chemically meaningful, we nonetheless demonstrate the applicability of X-CC to real electronic systems, which require accounting for exchange antisymmetry and inter-fragment charge transfer. The small size of these systems makes available a simple

(albeit inefficient) method to compute the excitonic Hamiltonian, which suffices for this proof-of-principle test. Failing an exact solution for more than just a few Be atoms, we compare our accuracy to conventional CCSD and CCSD(T), using these methods also as references for comparative timings.

## 4.1 Model Oscillator “Molecules”

This study considers an *a priori* pairwise fragment Hamiltonian of the following form, which is for generic closed systems of distinguishable internal coordinates, distributed in one dimension, and coupled only by the longitudinal dipole–dipole interaction

$$\hat{\mathcal{H}} = \sum_m \hat{H}^{(m)} + \sum_{m_1 < m_2} k^{(m_1, m_2)} \hat{\mu}^{(m_1)} \hat{\mu}^{(m_2)} \quad (7)$$

$\hat{H}^{(m)}$  is the Hamiltonian of fragment  $m$  in isolation, and  $\hat{\mu}^{(m)}$  is its dipole operator along the super-system axis. The coupling constant  $k^{(m_1, m_2)} = -(2E_h a_0)/(e^2 R_{m_1 m_2}^3)$  depends on the distance  $R_{m_1 m_2}$  between fragments  $m_1$  and  $m_2$ , where  $m_1 < m_2$  under the summation means to sum over all unique pairs.  $E_h$ ,  $a_0$ , and  $e$  are atomic units of energy, length and charge, respectively. Since the degrees of freedom are distinguishable, the tensor product set  $\{|\Psi_I\rangle\}$ , built from orthonormal sets of fragment states  $\{|\psi_{i_m}\rangle\}$ , is automatically an orthonormal basis for the super-system space. Considering separately the cases where, one, two, *etc.*, fragment states differ between the bra and ket of a matrix element, it is straightforward to show that the Hamiltonian projected into this super-system basis may be rewritten exactly as

$$\begin{aligned} \hat{\mathcal{H}} = & \sum_m \sum_{i_m, j_m} H_{j_m}^{i_m} \hat{\tau}_{i_m}^{j_m} + \sum_{m_1 < m_2} \sum_{\substack{i_{m_1}, j_{m_1} \\ i_{m_2}, j_{m_2}}} k^{(m_1, m_2)} \mu_{j_{m_1}}^{i_{m_1}} \mu_{j_{m_2}}^{i_{m_2}} \hat{\tau}_{i_{m_1}}^{j_{m_1}} \hat{\tau}_{i_{m_2}}^{j_{m_2}} \\ H_{j_m}^{i_m} = & \langle \psi_{i_m} | \hat{H}^{(m)} | \psi_{j_m} \rangle \quad \mu_{j_m}^{i_m} = \langle \psi_{i_m} | \hat{\mu}^{(m)} | \psi_{j_m} \rangle \end{aligned} \quad (8)$$

which intuitively has fragment rank of two. This Hamiltonian is in the form that we have demanded for the X-CC scheme.

It will be convenient to let each fragment be a group of linearly coupled harmonic oscillators, as a proxy for general internal interactions of fragment coordinates. If we further consider the coordinate of each primitive oscillator as representing the distance between two opposing

charges along the direction of the inter-fragment axis, then the dipole operators of the fragments are consequently defined. Such a model is convenient because the overall system is ultimately described by linear couplings between all pairs of primitive harmonic oscillators. Diagonalization of the system-wide matrix of coupling constants can be used to efficiently obtain the ground-state energy to within machine precision, for purposes of comparison. It should be made clear, however, that this method of exact solution relies on a special structure to the problem that is lost upon projection into a basis. The dimension of the basis-projected super-system Hamiltonian scales exponentially with  $N$ , and, furthermore, sparsity due to the dipolar selection rules is lost upon transformation to an internally correlated excitonic basis. Such systems are then reasonable mimics for the complexity of systems of real molecules. A Hamiltonian for weakly interacting molecules may also be written in the form of eq. (8).

Our test systems consist of linear chains of 2 to 30 oscillator-model “molecules,” equally spaced by either 5 or 10  $a_0$ . Each such fragment consists of 8 internal oscillators with force constants spread evenly over the range of 1 to 2  $E_h/a_0^2$ , inclusive. Each harmonic potential contains a particle with the same mass as an electron, and its coordinate is interpreted as the displacement of a  $-e$  charge, relative to one of  $+e$ . The coupling constant between each pair of internal oscillators has a positive (repulsive) value whose magnitude is 1/3 of the difference between their force constants, such that even oscillators with quite different force constants are substantially mixed in the fragment ground states. For the X-CC calculations we choose the set of internally correlated basis states  $\{|\psi_{i_m}\rangle\}$  for each fragment to be the set of exact energy eigenstates for each fragment in isolation, using the ground state of each fragment as its reference in the X-CC wavefunction. These fragment states, and the exact values of the corresponding matrix elements of  $\hat{H}^{(m)}$  and  $\hat{\mu}^{(m)}$ , are available via diagonalization of the *internal* coupling matrices for the individual fragments.

The accuracy and computational effort of the X-CC calculations will be compared to a CC calculation that operates on fluctuations of the primitive oscillators underlying the fragments. This is intended to mimic the conventional practice of working with creation and annihilation operators for individual electrons. Such a calculation is performed here as an X-CC calculation, but where each primitive oscillator is mapped to a fragment. An important aspect of this is that the same computer program can be used for both the excitonic and conventional/primitive CC calculations. Any efficiency advantage of X-CC can then be traced directly to the renor-

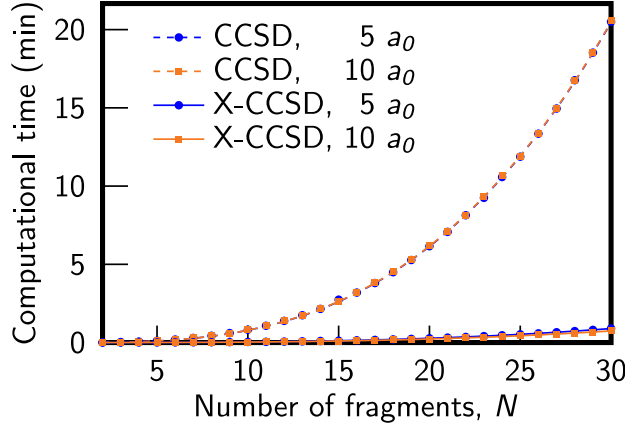


Figure 1: For either spacing between the oscillator-model “molecules,” the computational time for X-CCSD is much shorter than for an identically structured conventional CCSD algorithm. The best-fit connecting curves are described well as cubic functions.

	5 $a_0$		10 $a_0$	
	best-fit timing	asymptotic error	best-fit timing	asymptotic error
CCSD	$0.051 \times N^{2.97}$	$8.3 \times 10^{-4}$	$0.052 \times N^{2.96}$	$8.2 \times 10^{-4}$
X-CCSD	$0.0025 \times N^{2.94}$	$1.4 \times 10^{-6}$	$0.0021 \times N^{2.93}$	$3.2 \times 10^{-10}$

Table 1: X-CCSD is both more accurate and faster than conventional CCSD, for identically structured algorithms. For each spacing between the oscillator-model “molecules,” the best-fit monomial for the timing curve (in sec) is given along with the absolute error for large  $N$  (in  $E_h$ /fragment). Since X-CCSD does not need to account for internal fragment correlations, the error decays to zero with separation.

malization of the Hamiltonian, which shrinks the sizes of the tensors involved.

Given that only relative timings are important, the slower abstract implementation of the X2-CCSD amplitude equations suffices for this study (see appendix A). Since the Hamiltonian is manifestly pairwise, we suppress the “2” for the remainder of the discussion of these systems, as it does not constitute an approximation. In the limit that each primitive oscillator is nominally a fragment, the “X” is also suppressed, such that CCSD refers here to the primitive variant. For all calculations, convergence is declared when the energy correction changes by less than 1 part in  $10^8$  between iterations.

The computation times for CCSD and X-CCSD are plotted against the number of fragments in Fig. 1, for each inter-fragment spacing. All reported timings are for the smallest (fastest) calculation that converges to the inherent accuracy limit of the finite-order (X-)CCSD model (*i.e.*, the complete-basis limit); the determination of this convergence is discussed momentarily. The excitonic calculations are seen to be much faster than for the primitive variant, as reflected

in the best-fit monomials for each series, recorded in Table 1 (log–log least-squares regression for the largest 15 systems). These are consistent with our expectation of third-order scaling. The 20-fold decrease in the prefactor can be rationalized from the previously noted scalings as  $(1/8)^3(9/4)^4$  to account for the fact that the same algorithm is operating on 1/8 as many “fragments” (a fragment might be primitive oscillator), but with 9 states per fragment, instead of 4. Table 1 also gives the absolute error for the respective basis-converged calculations on the 30-fragment systems. This shows the excitonic variant to be not only faster, but also better. It is 3 orders of magnitude more accurate at 5  $a_0$  separation, and the error decays to zero with separation, since X-CC only needs to compute the interaction energy.

Determination of convergence with respect to basis size is assessed by observing the approach to the inherent method error as more states of increasing energy are considered for each subsystem (each fragment or each primitive oscillator). This limiting method error is due to the truncated excitation level in the (X-)CCSD wavefunction; it is different for the excitonic and primitive variants, and it depends on the inter-fragment spacing. Expressed as a fraction of the exactly known energy difference  $\Delta E$  that separates the ground state from the relevant (excitonic or primitive) reference, the method error is fairly independent of system size for the larger  $N$ . An asymptotic estimate of this constant unrecovered fraction of  $\Delta E$  was obtained by monitoring the error (with respect to the exact ground-state energy) for the 30-fragment system and declaring basis-set convergence when the order of magnitude and two significant figures of its ratio with  $\Delta E$  were stable. A few percent increase over this value was then established as a convergence threshold for this fraction, used for convenience to signal basis-set convergence for all other system sizes (of same spacing and CC variant). Irrespective of spacing or number of fragments, application of the aforementioned criterion uniformly demanded 9 states per fragment for the X-CCSD calculations and 4 states per oscillator for the CCSD calculations (*i.e.*, 32 states per fragment).

Table 2 gives the per-fragment value of the effectively asymptotic  $\Delta E$  (for 30 fragments), for each spacing and reference state. This value is much larger in the primitive case, where it represents the entire correlation energy, as opposed to only the inter-fragment interaction energy. The excitonic value therefore asymptotes to zero with increased separation, whereas the primitive value approaches a finite constant. Also given in Table 2 are the aforementioned threshold error fractions. In addition to the value of  $\Delta E$  being smaller when starting from an

	5 $a_0$		10 $a_0$	
	exact $\Delta E$	thresh. fraction	exact $\Delta E$	thresh. fraction
CCSD	$-5.0 \times 10^{-2}$	$1.7 \times 10^{-2}$	$-4.9 \times 10^{-2}$	$1.7 \times 10^{-2}$
X-CCSD	$-5.5 \times 10^{-4}$	$2.6 \times 10^{-3}$	$-8.5 \times 10^{-6}$	$4.2 \times 10^{-5}$

Table 2: For the oscillator-model “molecules,” the energy change  $\Delta E$  (in  $E_h$ /fragment) to reach the ground state, from either a primitive (CCSD) or excitonic (X-CCSD) reference state, is given for large  $N$ . The threshold fraction of  $\Delta E$  that is unrecovered near convergence to the complete basis limit is also given. X-CCSD recovers a larger fraction of an already smaller energetic distance to the ground state.

excitonic reference, X-CCSD leaves a smaller fraction of this already smaller energetic distance to the ground state unrecovered. Note that the product of each pair of  $\Delta E$  and threshold-fraction values in Table 2 is, in fact, a slight overestimate of the respective absolute error reported in Table 1.

## 4.2 Beryllium-atom Chains

This study performs tests of the X2-CCSD model using simple electronic fragments. These are Be atoms in a 6-31G basis, with the core electrons frozen in the Hartree–Fock 1s orbitals of the isolated atoms. The neutral fragments are effectively 2-electron ( $2e^-$ ) problems, and the basis set here is too small for chemically meaningful results. However, our purpose is only to set up a model problem that has all the essential features of fragment-decomposed electronic systems: inter-fragment electron exchange, charge transfer, and strong intra-fragment correlations. Accuracy is defined relative to the (hypothetical) FCI solution of the basis-projected problem.

It is worth noting for context that the Be dimer is already a notoriously difficult multi-reference problem, which has received much attention over several decades.<sup>40–47</sup> This is ultimately due to the fact that the two valence electrons of each atom live in a space of four nearly degenerate orbitals; this leads to substantial angular correlation (evident even in a 6-31G basis<sup>48</sup>). The dimer bonding curve has a long-appreciated odd shape, which illuminatingly separates into two distinct minima in FCI calculations as the basis size is decreased from cc-pVTZ to cc-pVDZ. The deeper inner minimum eventually converges (with basis quality) to the observed dissociation depth of roughly 4  $mE_h$  (10 kJ/mol) at the equilibrium bond length, near 2.5 Å. The shallower outer minimum, near 4.5 Å, eventually merges in to form a noticeable

shoulder of the binding well. Only this outer minimum is captured using the 6-31G basis.

Unlike for the study of the oscillator “molecules,” the basis for the primitive (one-electron) coordinates is a fixed feature of these simulations. Although this is removed as a variable from the discussion of the conventional CC results, one of the most important remaining considerations is the *many-electron* basis used for each atomic fragment in the X-CC calculations. Indeed, the decision to use such a small one-electron basis is driven by the desire to allow a nimble exploration of this crucial facet.

The conceptually simplest scheme for choosing fragment states is that used for the oscillator systems, systematically increasing the number of fragment energy eigenstates considered. There are two difficulties with this approach that could easily be anticipated, even assuming that FCI on the fragments were not an issue. These were indeed both met in practice. The first is that prioritizing states on the basis of their energy alone ignores the equally important consideration of the coupling strengths; some low-energy atomic states will be unimportant to inter-fragment interactions, whereas some high-energy states will couple strongly. The second is that, even for nominally non-covalent interactions, some charge transfer will be important; consider the quintessential example of the semi-covalent hydrogen bond.<sup>49</sup> Recovering this interaction would involve converging also cationic and anionic eigenstates of the fragments. The anionic states will be particularly problematic if the anionic fragment is not stable. However, in the field of a nearby electron hole, such states can contribute. As an easily accessible example, consider that the Li<sub>2</sub> bond is described by substantial two-center electron resonance, in spite of the small electron affinity of Li.

A reasonable manner in which to circumvent both of the forgoing issues, at least theoretically, is to work “backwards,” identifying those atomic states of greatest import for the nearest-neighbor interaction, and then using these states for the global problem. The essential tool for this is the construction of a density matrix in the single-fragment many-electron Fock space. Working with such small fragments here, we can do this by brute force. An FCI calculation is first performed on a dimer at 4.5 Å, using a primitive in-house program that either builds the Hamiltonian matrix explicitly or allows for eigenvector extraction with the Lanczos<sup>50</sup> algorithm. This ground state is then resolved in terms of the complete set of anti-symmetrized tensor products of atomic states, numbering 16 cationic (1e<sup>-</sup>), 120 neutral (2e<sup>-</sup>), and 560 anionic (3e<sup>-</sup>) states for each atom. The 1820 possible dianionic (4e<sup>-</sup>) states in this

basis (requiring the transfer of both active electrons from one atom to the other) were excluded from this resolution. Since we insist that the contribution of  $4e^-$  atomic states is negligible (verified later), to declutter the terminology, we refer to the union of the  $1e^-$ ,  $2e^-$ , and  $3e^-$  spaces of active electrons on each atom as the full Fock space of that atom. The states that we used for this resolution of the dimer ground state were, in fact, the atomic energy eigenstates (anionic states trapped by the basis). This means that we already have the single-fragment Hamiltonian in diagonal form for later. As a detail, a preliminary step resolved the eigenstates of each atom in terms of the dimer molecular orbitals, such that antisymmetrization of the tensor products simply requires the Pauli exclusion principle. The tensor-product basis of atomic states is not orthonormal, but the coefficients nevertheless reflect the relative importance of individual atomic states. To simplify interpretation before further processing, this projected *vector* is scaled to have unit norm (as opposed to the state it represents, which is now not normalized).

We can now algorithmically identify most important atomic states. By interpreting the renormalized ground-state resolution as if it referred to an *orthonormal* tensor-product basis, a full Fock-space density matrix is constructed for both the “left” and the “right” atom, denoted  $\rho_L$  and  $\rho_R$ , each having unit trace. In order to avoid any left–right bias of the fragment states these density matrices were averaged as  $\rho = (\rho_L + \rho_R)/2$ . The eigenvectors of  $\rho$  are now the coefficients of a set of fragment states  $\{|\psi'_{i_m}\rangle\}$ , where  $m$  is any one of the identical fragments. Each member of this basis is accompanied by an associated probability eigenvalue  $\rho_{i_m}$ . Our criterion for constructing the X-CC fragment basis  $\{|\psi_{i_m}\rangle\}$  is to simply select the subset of  $\{|\psi'_{i_m}\rangle\}$  whose members each have  $\rho_{i_m} > 10^{-6}$ . This threshold is relatively arbitrary, chosen only to provide an accuracy for the dimer that is beyond reproach, while still demonstrating the efficiency of the method for larger systems. Application of this threshold chooses only 23 states for each atom from their respective 696-dimensional Fock spaces; 11 of these are neutral states, while 4 are cationic, and 8 are anionic. These states, obtained for a dimer at 4.5 Å separation, are the fixed basis for all Be fragments going forward, regardless of their number or the distance between them.

With the model space for each fragment now fixed, the corresponding excitonic Hamiltonian is also defined, in principle, per the discussion of fragment-decomposed electronic systems provided in the companion article. In practice, however, we may apply further approximations.

Already mentioned among these is the neglect of the trimer and tetramer terms in the X2-CCSD Hamiltonian. We should also carry along some indication of the scheme by which the fragment states are determined, but we suppress this presently, since the Hamiltonian is effectively converged in this respect (verified later), and a systematic taxonomy has not been developed. Yet another approximation will be made here by assuming that the dimer coupling elements for any pair of fragments are independent of the presence of other fragments. We augment the method name here as X2'-CCSD to reflect this. The reason for applying this approximation is only to simplify the programming tasks necessary to complete this proof-of-principle demonstration. Although intuitive (and exact for two-fragment systems), this assumption effectively relaxes global antisymmetry. We expect the effect of this to be small here, due to the large inter-fragment spacing. Also, removing it would involve substantially more programming, but, per the discussion in the companion article, the result is still an asymptotically quadratic computational step. We postpone the exposition of the exact procedure used to construct the Hamiltonian here to the end of this discussion.

For these calculations, the faster, explicit version of the X2-CCSD amplitude equations was implemented (see appendix A). With the further use of a threshold on the Hamiltonian matrix elements, requiring only a few human programming hours, this computer code was also sped up dramatically, so much that it even lowers the scaling, while preserving the results to within machine precision. Further discussion of this takes place after the results are presented. It is worth mentioning that Psi4 similarly applies a threshold to the one- and two-electron integrals with which it operates. Ultimately, our purpose here, however, is only to provide evidence that X-CC is a promising approach when measured against a state-of-the-art standard, not to instigate a competition against any specific conventional CC implementation or input deck. For all calculations, both X2'-CCSD and conventional [henceforth, just CCSD or CCSD(T)], the coupled-cluster iterations converged when the total energy changed by less than  $10^{-12} E_h$  between iterations. This is an observation, rather than a criterion, though thresholds in each code were adjusted to arrange for this agreement.

Fig. 2 shows dissociation curves for the dimer and symmetric linear trimer. The nearly exact agreement of X2'-CCSD with FCI for the dimer is essentially by construction. Firstly, the wavefunction is complete. Secondly, the restriction to dimer terms in the Hamiltonian does not constitute an approximation, and the subsequent implied relaxation of global antisymmetry

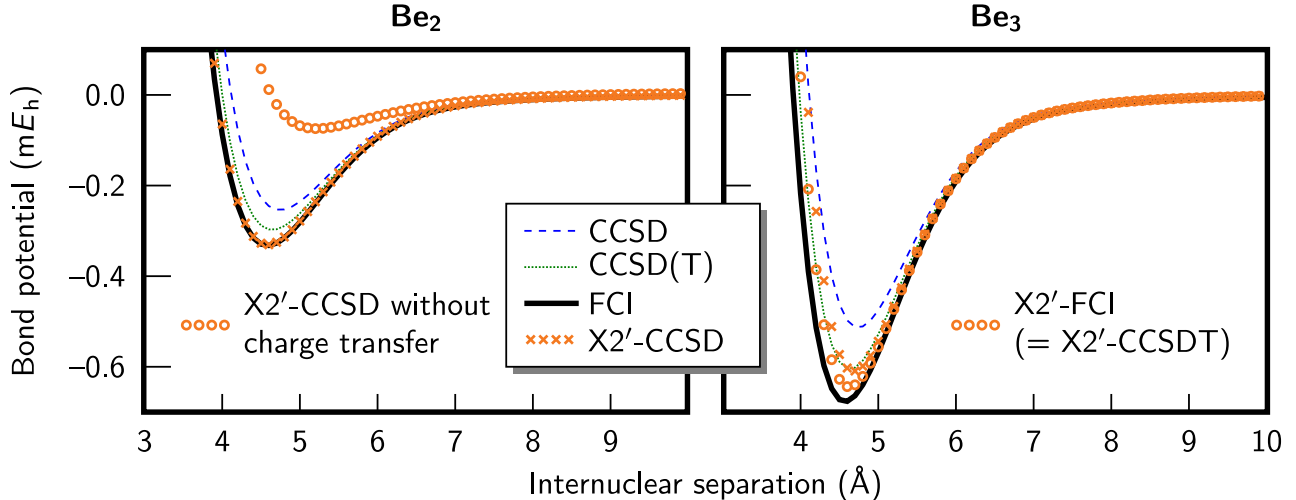


Figure 2: The accuracy of X2'-CCSD is comparable to FCI and CCSD(T) for the dimer and symmetric linear trimer, respectively. Note that the inclusion of charge-transfer fluctuations (*i.e.*, different charge states for the fragments) is important for recovering the interaction. By way of analyzing sources of error (Hamiltonian vs. wavefunction), a complete wavefunction was tested for the approximate trimer Hamiltonian, accounting for roughly half of the discrepancy against FCI. X2'-CCSD is exact by construction for the dimer at 4.5 Å.

is exact for dimers. Thirdly and finally, the single-fragment basis was chosen to render the excitonic effective Hamiltonian numerically converged with respect its description of the ground-state dimer (at least, at 4.5 Å). For reference, CCSD and CCSD(T) curves show that, in spite of the small system size, this nearly exact agreement is not to be taken for granted. One of the most interesting aspects of the dimer plot is the X2'-CCSD calculation that omits anionic and cationic states, effectively suppressing charge transfer. It is primarily interesting that such a model is so easily defined, and it hints at the possible utility of X-CC approaches to provide insight into bonding character and basis-set superposition error. It also validates our earlier claim that charge transfer is important for these test systems (at least, in this basis), and it provides a numerical demonstration that X-CC is equipped to handle such problems.

The trimer curve in Fig. 2 shows that the accuracy does diminish when the dimer-restricted Hamiltonian and wavefunction are applied to a trimer system. There are four possible sources of error here. The first possibility is the truncated wavefunction. To test this, we would like to run an X2'-CCSDT calculation; however, in lieu of deriving the amplitude equations for this, we perform an equivalent X2'-FCI calculation. The excitonic Hamiltonian is used to populate a Hamiltonian matrix in terms of the hypothetical biorthogonal super-system basis states (which need not be constructed, only indexed). Indeed, a substantial fraction of the error is owed to

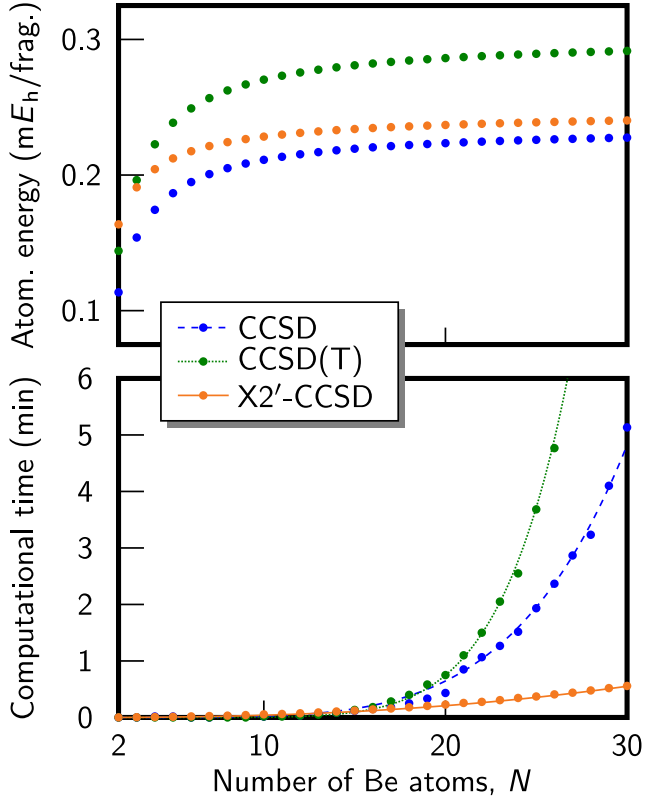


Figure 3: The atomization energy (per fragment) and computational effort for each method are plotted for linear chains of Be atoms. The accuracy of X2'-CCSD is comparable to CCSD for the larger systems, but the computational effort is much smaller. The connecting curves are best-fit monomials; these scale as  $\sim N^{2.40}$ ,  $\sim N^{4.96}$ , and  $\sim N^{7.19}$ , for X2'-CCSD, CCSD, and (T), respectively. For CCSD(T), only the time for the perturbative triples (T) module is plotted.

missing trimer correlations.

The remaining possible errors in the trimer calculations stem from approximations applied to the Hamiltonian. Foremost, the Hamiltonian is missing trimer terms, and we have made further approximations that allow for implicit global antisymmetry violations. Only implementation of the fully antisymmetric excitonic Hamiltonian will be able to discern the relative sizes of these two errors. The former seems likely to be substantial, since the electrostatic effects on one atom from a nearby disjoint charge transfer are neglected. Theoretically, there is also the possibility that the single-fragment states optimized for nearest-neighbor interactions are not appropriate for capturing next-nearest neighbor interactions. This would be unexpected, since the dimer dissociation curve was so accurate over such a large range, but there could be a non-trivial end-to-end interaction mediated by the middle atom.<sup>33,51</sup> To test, we lowered the threshold on the values of the  $\rho_{i_m}$  to  $10^{-7}$ , and this lowers the dissociation minimum by only

$N$	time (min)
10	0.1
20	0.2
30	0.6
40	1.1
50	1.9
60	2.8
70	4.2
80	5.7
90	7.8
100	10.6

Table 3: Single-core computational times are given for the X2'-CCSD algorithm for linear chains of  $N$  Be atoms. The time for assembling the Hamiltonian (a quadratically scaling step) is not included.

0.8  $\mu E_h$ . So this appears not to contribute significantly to the error.

Since X2'-CCSD agrees with FCI for the dimer but only roughly CCSD(T) for the trimer, the next natural question is whether the quality continues to degrade. To answer this question, the atomization energies of chains of up to 30 atoms (4.5 Å separation) are plotted in Fig. 3, along with the same quantity computed using CCSD and CCSD(T). The error does level off when reckoned per fragment, and the quality is always a little better than for CCSD.

Having verified that the X2'-CCSD method is at least as good as CCSD in terms of absolute accuracy for any given system, we turn to computational cost. The run times for systems of up to 30 atoms are plotted in Fig. 3. X2'-CCSD is not only faster already for modest  $N$ , but it has a lower scaling. The best-fit monomials have exponents of 2.40, 4.96, and 7.19 for X2'-CCSD, CCSD, and the perturbative triples module (T), respectively (log–log least-squares regression for the largest 10 systems). Whereas these exponent estimates are still rather sensitive to the range chosen for CCSD and (T), indicating more general polynomial behavior, X2'-CCSD (generally, X2-CCSD) has largely reached its asymptotic scaling. This was verified by fitting to timings for up to 100 atoms, obtaining an exponent of 2.29 over this range. Timings for these calculations are given in Table 3. Notably, a calculation involving 200 active electrons in 800 spatial orbitals has been completed in just 10.6 min, at roughly CCSD accuracy.

The scaling of the X2-CCSD code is below the formally expected third-order behavior due to the thresholding of the Hamiltonian matrix elements. Those elements smaller than  $10^{-16} E_h$  were discarded by setting them to explicit floating-point zero before the wavefunction iterations.

To the maximum extent possible, the tensor contractions had been arranged to have the loop over the Hamiltonian indices on the outside of any nesting. The code could then be made more efficient by simply testing on the fly whether each Hamiltonian element is identically zero. The massive sparsity of the excitonic Hamiltonian for large systems more than compensates for this extra test. The fact that such dramatic improvement can be rendered so easily speaks well of the *a priori* use of locality in the X-CC model. Since optimization is still largely a work in progress, we postpone a thorough discussion to a future publication, except to report that, for thresholds in the regime of  $10^{-12}$  to  $10^{-16}$   $E_h$ , the X2'-CCSD energy is unchanged to within machine precision, and the timing curves do not differ substantially. This hints that the majority of discarded elements are actually very much smaller than the threshold. For the record, the Psi4 calculations neglected integrals smaller than  $10^{-12}$   $E_h$ .

We now finally elucidate the procedure undertaken here for construction of the “X2” excitonic Hamiltonian. Our brute force procedure for identifying the most important single-fragment states leaves us with dimer coupling information already at hand. Using the resultant  $696 \times 23$  monomer transformation matrix, we transform the  $(696 \cdot 696) \times (696 \cdot 696)$  dimer Hamiltonian matrix in the non-orthonormal full tensor-product basis to a  $(23 \cdot 23) \times (23 \cdot 23)$  projection thereof, where the basis is again not orthonormal. Interestingly, while this projection is block-diagonal by electron number, it does contain blocks for 2 through 6 active electrons. These are all necessary; although each fluctuation in  $\hat{T}$  conserves *overall* charge, these fluctuations interact, and atoms that may have changed charge state in their interaction with one atom can interact with yet another. Per the discussion in the companion article, antisymmetry in the X-CC formalism is accounted for by representing the Hamiltonian matrix elements in a biorthogonal basis. This is accomplished here for the dimer terms by multiplication of the raw Hamiltonian projection by the inverse of the  $(23 \cdot 23) \times (23 \cdot 23)$  overlap matrix for the tensor-product basis of the retained fragment states. Meanwhile, the  $23 \times 23$  Hamiltonian for an isolated fragment is trivially obtained from the 696 known fragment eigenenergies. In order to isolate the dimer *coupling* elements, the tensor product of the single-fragment Hamiltonian matrix with itself (to represent the second identical fragment) is subtracted from the dimer Hamiltonian matrix. Subtractive steps such as this are unnecessary in the exact procedure given in the companion article.

## 5 Conclusion

In this article, we have laid out the theory and prospective advantages of basing a CC wavefunction on fluctuations of fragments between internally correlated states. Two numerical demonstrations of the promise of this approach have been provided.

As respects application to more chemically interesting systems, it should be pointed out that, in some ways, the simulations performed here were already demanding. The entire interaction between two Be atoms in the basis employed is on the order of 1 kJ/mol, the often-stated threshold for chemical accuracy, and our absolute errors were small percentages of this. Furthermore, with such a small excitation energy (2.7 eV, as compared to 7.5 eV for water<sup>52,53</sup>), the Be atom is quite polarizable ( $38 e^2 a_0^2 / E_h$ , as compared to  $10 e^2 a_0^2 / E_h$  for water<sup>54,55</sup>). The only variables, aside from system size, that determine the computational cost of a given X-CC variant are the number of states per fragment and the sparsity of the couplings in that basis. At present, it is difficult to know if, for example, coupled water molecules in a high-quality one-electron basis will require much greater than 23 many-electron states per fragment. In case only 23 states were needed, however, then the X2-CCSD cost for 100 water molecules would be the same as for the 100-Be-atom system, namely  $\sim$ 11 min (presuming similar Hamiltonian sparsity); the extrapolation to 1000 such fragments is 1.5 days.

The timings here are for a computer program that is not yet very sophisticated, or even parallelized, so there is plenty of room for optimism. Similar to familiar local-correlation methods,<sup>56–60</sup> hard-coded assumptions about the way interactions behave over large distances can greatly improve efficiency.

An important aspect of the X-CC model is that it is theoretically independent of the level of electronic structure theory used to compute the fragment states. Since X-CC is not tied to any specific level of theory, it is not inherently subject to the shortcomings of any given base method. The level of theory used for individual fragments could even be multi-reference in nature, effectively inverting the traditional paradigm of introducing dynamic correlation into multi-reference problems.<sup>61–66</sup> The treatment of a super-system also need not be spatially homogeneous; fewer states of lower quality may be used farther from a region of interest. Yet, the rigor of the formalism renders all of this systematically improvable. Naturally, the flexibility to have the entire quantum mechanical system subject to an external potential (*e.g.*, molecular mechanics embedding) is still available.

The excited-state regime may also be accessed via the established equation-of-motion formalism for linear response.<sup>67,68</sup> The ability to straightforwardly proceed from ground-state to excited-state calculations, on account of having a global wavefunction, is an important distinction, in contrast to incremental methods,<sup>12,13,69</sup> which are formally exact fragment decompositions of the ground-state energy and properties only.

Work in the immediate future will apply the X-CC algorithm to the more carefully implemented excitonic Hamiltonians detailed in the companion article, including exact treatment of global (as opposed to pairwise) antisymmetry. In that article, it was shown that, to within an arbitrary threshold, the number of terms in the exact excitonic Hamiltonian scales asymptotically quadratically with system size. There will admittedly be cases where the cost of constructing this Hamiltonian is prohibitive, but also a number of important cases where it is not. More tractable schemes of determining a preliminary single-fragment basis also need to be developed to facilitate this, though it is important to note the continued availability of algorithmic optimizations of the single-fragment bases. To be concrete, the X-CC energy is differentiable with respect to fragment-basis rotations, and optimization could be done in advance for dimers only, similar to what was done here.

## Acknowledgements

The authors gratefully acknowledge start-up support from the Hornage Fund at the University of the Pacific, as well as equipment and travel support provided by the Dean of the College of the Pacific. The following colleagues are recognized for useful insights during the development of this work: Arindam Chakraborty, Gregory J. O. Beran, Oriol Vendrell, Andreas Dreuw, Joshua Schrier.

# Appendix

## A Amplitude Equations

There are aspects of the excitonic CC amplitude equations which are both more and less complex than the conventional CC equations. On the one hand, the Hamiltonian may contain up to four-fragment (four-body) interactions, and Wick’s theorem must first be generalized for the situation where “creation” and “annihilation” indices are always found as paired, in order to build a diagrammatic algebra. On the other hand, each such pair references two states of the same fragment, and no operator string in the Hamiltonian or cluster operator contains more than one fluctuation operator referencing any given fragment. This ultimately provides a simplification of the brute-force algebraic approach, which we pursue here.

Before proceeding, it is worthwhile to note that the above simplifying conditions effectively allow the excitonic Hamiltonian to be mapped onto one for distinguishable particles. The many-body states of each fragment can be mapped onto the one-body states of some fictitious particle. Pairs of field operators that annihilate and create particles in those states then serve as mappings for the fluctuation operators. For example, an excitonic Hamiltonian for  $N$  fragments can be mapped onto an  $N$ -mode vibrational problem. We therefore expect the same computational complexity here as for vibrational CC (VCC) theory, for which the nomenclature VCC[ $n$ ] is used to indicate that up to  $n$ -fold connected substitutions occur in the wavefunction. Indeed the  $N^3$  computational scaling that will be arrived at here is the same as for VCC[2] for Hamiltonians with two-mode couplings.<sup>70</sup> Nevertheless, we wish to show that the amplitude equations can be derived here solely from the commutator in eq. (3), without the tertiary step of introducing such a mapping to vibrations.

It is also worthwhile to point out that fermionic problems can be directly mapped to excitonic (and therefore vibrational) problems directly, by letting each orbital be a two-state system (occupied or not). The conventional CCSD wavefunction then maps onto VCC[4] with four-mode couplings, for which the computational scaling is  $N^6$ , as expected. This strongly suggests that algorithmic complexity is conserved across CC mappings, and that X3-CCSD and X4-CCSD should have the  $N^3$  and  $N^4$  formal scalings of three- and four-mode VCC[2], respectively. We will also later have need of the reverse mapping of an excitonic problem into

a fermionic problem, as part of our program validation chain. Here, every fragment state is represented by an orbital, but only transitions within disjoint orbital subsets (for distinct fragments) are allowed. This is inefficient, as it leads to very sparse mapped integrals tensors, but it allows conventional CC codes to run excitonic calculations.

We now begin by defining operators that have properties closely related to the normal ordering of field operators (under the mapping  $\hat{\tau}_i^j \rightarrow \hat{a}_i^\dagger \hat{a}_j$ ).

$$\begin{aligned}\hat{e}_{u_m}^{o_m} &= \hat{\tau}_{u_m}^{o_m} \\ \hat{f}_{o_m}^{o_m} &= 1 - \hat{\tau}_{o_m}^{o_m} \\ \hat{f}_{u_m}^{v_m} &= \hat{\tau}_{u_m}^{v_m} \\ \hat{d}_{o_m}^{u_m} &= \hat{\tau}_{o_m}^{u_m}\end{aligned}\tag{9}$$

Any operator originally expressed in terms of the set of fluctuation operators  $\{\hat{\tau}_i^j\}$  may be expressed in terms of these new operators by simple substitution. The indices  $u_m, v_m, w_m, x_m$  refer to any state of fragment  $m$  except the reference state, which is denoted  $o_m$ . These letters have been chosen to be reminiscent of the “occupied” and “unoccupied/virtual” nomenclature familiar from conventional many-body theory, and yet be distinct from its usual notation. Similarly, the letters used for the four different types of operators stand for “excitation,” “flat,” and “de-excitation.”

Of primary importance is that all such operators, except excitations, produce the null state when acting on the many-fragment reference. In general, it will be valuable to consider a generalized definition of normal ordering for strings of such operators, in which any excitation operators appear to the left of all other operators. In this way, any normal-ordered string will destroy the reference state unless it contains only excitations (or is a scalar). For  $\hat{\mathcal{H}}$ , this is trivial to accomplish; since no string therein contains more than one operator that acts on any given fragment, all operators in these strings commute. The substitution of  $\hat{\tau}_{o_m}^{o_m}$  by  $1 - \hat{f}_{o_m}^{o_m}$  does introduce a constant into the normal-ordered Hamiltonian, however, which is equal to  $\langle \Psi^O | \hat{\mathcal{H}} | \Psi_O \rangle$ , in analogy to the conventional normal-ordered Hamiltonian in terms of field operators.

The cluster operator  $\hat{T}$ , which must be repeatedly commuted with  $\hat{\mathcal{H}}$ , is composed only of operators of the excitation class. The following special cases of the commutator in eq. (3) will

therefore be useful

$$\begin{aligned}
[\hat{e}_{u_m}^{o_m}, \hat{e}_{w_m}^{o_m}] &= 0 \\
[\hat{f}_{o_m}^{o_m}, \hat{e}_{w_m}^{o_m}] &= \hat{e}_{w_m}^{o_m} \\
[\hat{f}_{u_m}^{v_m}, \hat{e}_{w_m}^{o_m}] &= \delta_{v_m w_m} \hat{e}_{u_m}^{o_m} \\
[\hat{d}_{o_m}^{u_m}, \hat{e}_{w_m}^{o_m}] &= \delta_{u_m w_m} - (\delta_{u_m w_m} \hat{f}_{o_m}^{o_m} + \hat{f}_{w_m}^{u_m})
\end{aligned} \tag{10}$$

where we recall that commutators between operators belonging to different fragments are always zero. This now makes explicit earlier arguments concerning truncation of the BCH expansion, in that repeated commutations of any operator with excitations always ends with zero. No operator survives more than two such nested commutations.

In order to be generic at some points, we will let  $\hat{g}_m$  represent an arbitrary single-fragment operator on fragment  $m$ . This could be any one of  $\hat{e}_{u_m}^{o_m}$ ,  $\hat{f}_{o_m}^{o_m}$ ,  $\hat{f}_{u_m}^{v_m}$ , or  $\hat{d}_{o_m}^{u_m}$ , or linear combinations thereof, and we permit this notation to also include linear combinations that contain constants. We then furthermore define the abbreviations

$$\begin{aligned}
\hat{g}_m^{[w_m]} &= [\hat{g}_m, \hat{e}_{w_m}^{o_m}] \\
\hat{g}_m^{[w_m][x_m]} &= [[\hat{g}_m, \hat{e}_{w_m}^{o_m}], \hat{e}_{x_m}^{o_m}]
\end{aligned} \tag{11}$$

noting that these are themselves single-fragment operators (for purposes of recursion). According to forgoing observation, all nested commutations higher than second order are zero. Using this notation, combined with recursion of the well-known formula for commutation with a simple operator product, we then resolve commutation of a single-fragment operator with a string of  $M$  excitations as

$$[\hat{g}_m, \hat{e}_{w_{m_1}}^{o_{m_1}} \cdots \hat{e}_{w_{m_M}}^{o_{m_M}}] = \sum_{i=1}^M \delta_{m, m_i} \hat{e}_{w_{m_1}}^{o_{m_1}} \cdots \hat{e}_{w_{m_{(i-1)}}}^{o_{m_{(i-1)}}} \hat{e}_{w_{m_{(i+1)}}}^{o_{m_{(i+1)}}} \cdots \hat{e}_{w_{m_M}}^{o_{m_M}} \hat{g}_m^{[w_{m_i}]} \tag{12}$$

under the condition that the indices  $m_1, \dots, m_M$  identify distinct fragments, thus allowing rearrangement of the operator strings. Also, under this restriction, maximally one term of the right-hand side of eq. (12) is nonzero.

The  $M$ th-order part of the cluster operator can be written as

$$\begin{aligned}\hat{T}_M &= \sum_{m_1} \sum_{m_2 > m_1} \cdots \sum_{m_M > m_{M-1}} \left( \sum_{w_{m_1}} \cdots \sum_{w_{m_M}} t_M^{w_{m_1} \cdots w_{m_M}} \hat{e}_{w_{m_1}}^{o_{m_1}} \cdots \hat{e}_{w_{m_M}}^{o_{m_M}} \right) \\ &= \frac{1}{M!} \sum_{m_1} \cdots \sum_{m_M} \left( \sum_{w_{m_1}} \cdots \sum_{w_{m_M}} t_M^{w_{m_1} \cdots w_{m_M}} \hat{e}_{w_{m_1}}^{o_{m_1}} \cdots \hat{e}_{w_{m_M}}^{o_{m_M}} \right)\end{aligned}\quad (13)$$

where the total cluster operator  $\hat{T} = \sum_M \hat{T}_M$  is a summation over all orders  $M \geq 1$  present in the Ansatz. In the first line, we sum over all unique  $M$ -tuples of fragments, and in the second line we account for redundancy by dividing by  $M!$  and insisting that the tensor of amplitudes  $\mathbf{t}_M$  (containing elements  $t_M^{w_{m_1} \cdots w_{m_M}}$ ) is invariant with respect to all index permutations. We may also insist that an amplitude is zero if any two indices belong to the same fragment, effectively removing from further consideration those operator strings in which the same fragment occurs twice (though this is not strictly necessary, since such strings themselves contribute zero). Using eq. (12), we then arrive at

$$\begin{aligned}[\hat{g}_m, \hat{T}_M] &= \frac{1}{M!} \sum_{m_1} \cdots \sum_{m_M} \left( \sum_{w_{m_1}} \cdots \sum_{w_{m_M}} t_M^{w_{m_1} \cdots w_{m_M}} [\hat{g}_m, \hat{e}_{w_{m_1}}^{o_{m_1}} \cdots \hat{e}_{w_{m_M}}^{o_{m_M}}] \right) \\ &= \frac{1}{(M-1)!} \sum_{m_1 \neq m} \cdots \sum_{m_{M-1} \neq m} \left( \sum_{w_{m_1}} \cdots \sum_{w_{m_{M-1}}} \sum_{w_m} t_M^{w_{m_1} \cdots w_{m_{M-1}} w_m} \hat{e}_{w_{m_1}}^{o_{m_1}} \cdots \hat{e}_{w_{m_{M-1}}}^{o_{m_{M-1}}} \hat{g}_m^{[w_m]} \right) \\ &= \sum_{w_m} \hat{T}_{M-1}^{w_m} \hat{g}_m^{[w_m]} \\ \hat{T}_M^{w_m} &= \frac{1}{M!} \sum_{m_1 \neq m} \cdots \sum_{m_M \neq m} \left( \sum_{w_{m_1}} \cdots \sum_{w_{m_M}} t_{M+1}^{w_{m_1} \cdots w_{m_M} w_m} \hat{e}_{w_{m_1}}^{o_{m_1}} \cdots \hat{e}_{w_{m_M}}^{o_{m_M}} \right) \\ &= \frac{1}{M!} \sum_{m_1} \cdots \sum_{m_M} \left( \sum_{w_{m_1}} \cdots \sum_{w_{m_M}} t_{M+1}^{w_{m_1} \cdots w_{m_M} w_m} \hat{e}_{w_{m_1}}^{o_{m_1}} \cdots \hat{e}_{w_{m_M}}^{o_{m_M}} \right) \\ \hat{T}_0^{w_m} &= t_1^{w_m}\end{aligned}\quad (14)$$

The logical process by which this is deduced is to decompose each of the  $M$  summations over all fragments in the first line into one component for fragment  $m$  and a summation over all fragments other than  $m$ . This gives a total of  $2^M$  terms when the resulting  $M$ -fold binomial product is expanded. Only  $M$  of these terms survive, since the relevant amplitude is zero if any two indices both belong to fragment  $m$  and the commutator is zero if no fragment index is equal to  $m$ ; therefore, only one fragment can be equal to  $m$  in any surviving term, of which

there are  $M$  choices. Each surviving term contains  $M - 1$  summations over the other fragments. Since all of the other fragments and indices are summed over, and since all of the operators in the strings commute and amplitudes are permutationally symmetric, these  $M$  terms are all identical, simply reducing the prefactor to  $1/(M - 1)!$  for the single such term written explicitly in the second line. In the last line, the restrictions on the summations are removed since the amplitudes of the superfluous terms thereby introduced are zero. This has the advantage of giving  $\hat{T}_M^{w_m}$  an identical structure to  $\hat{T}_M$  (for  $M \neq 0$ ), but with different amplitudes, permitting us to use recursion to immediately write

$$\begin{aligned} [\hat{g}_m, \hat{T}_M^{w_m}] &= \sum_{w_m} \hat{T}_{M-1}^{w_m w_m} \hat{g}_m^{[w_m]} \\ \hat{T}_M^{w_m w_m'} &= \frac{1}{M!} \sum_{m_1} \cdots \sum_{m_M} \left( \sum_{w_{m_1}} \cdots \sum_{w_{m_M}} t_{M+2}^{w_{m_1} \cdots w_{m_M} w_m w_{m'}} \hat{e}_{w_{m_1}}^{o_{m_1}} \cdots \hat{e}_{w_{m_M}}^{o_{m_M}} \right) \\ \hat{T}_0^{w_m w_m'} &= t_2^{w_m w_{m'}} \end{aligned} \quad (15)$$

Eq. (15) will be necessary later to bring the transformation of products of operators into generalized normal-ordered form.

It will now be expedient to define the following summations over  $M$ , in parallel to the definition of  $\hat{T}$  itself

$$\begin{aligned} \hat{T}^{w_m} &= \sum_M \hat{T}_{M-1}^{w_m} \\ \hat{T}^{w_m w_m'} &= \sum_M \hat{T}_{M-2}^{w_m w_m'} \end{aligned} \quad (16)$$

where the summation over  $M$  is over all orders originally in the user Ansatz. (For consistency, both  $\hat{T}_M^{w_m}$  and  $\hat{T}_M^{w_m w_m'}$  are defined as zero for  $M < 0$ .) These allow us to write more compactly

$$\begin{aligned} [\hat{g}_m, \hat{T}] &= \sum_{w_m} \hat{T}^{w_m} \hat{g}_m^{[w_m]} \\ [\hat{g}_m, \hat{T}^{w_m'}] &= \sum_{w_m} \hat{T}^{w_m w_m'} \hat{g}_m^{[w_m]} \end{aligned} \quad (17)$$

By recursion, we then also arrive at

$$[[\hat{g}_m, \hat{T}], \hat{T}] = \sum_{w_m} \sum_{x_m} \hat{T}^{w_m} \hat{T}^{x_m} \hat{g}_m^{[w_m][x_m]} \quad (18)$$

where it is clear that any triply nested commutator vanishes. This allows us to then use the BCH expansion to finally write, for any single-fragment operator,

$$\bar{g}_m = e^{-\hat{T}} \hat{g}_m e^{\hat{T}} = \hat{g}_m + \sum_{w_m} \hat{T}^{w_m} \hat{g}_m^{[w_m]} + \frac{1}{2} \sum_{w_m} \sum_{x_m} \hat{T}^{w_m} \hat{T}^{x_m} \hat{g}_m^{[w_m][x_m]} \quad (19)$$

where the abbreviation as  $\bar{g}_m$  will be convenient later. Importantly, as a consequence of the restrictions on the indices in  $\hat{T}$  referring to distinct fragments in each string, each term in this expansion is already in the aforementioned generalized normal-ordered form.

The forgoing suffices to perform the similarity transformation of the single-fragment parts of  $\hat{\mathcal{H}}$ , and it can also be used to construct expressions for the higher-fragment-order terms. In order to proceed with the latter task, we first note that any operator  $\hat{o}$  may be decomposed as  $(\hat{o})_x + (\hat{o})_o$ , such that,

$$\begin{aligned} (\hat{o})_x |\Psi_O\rangle &= \hat{o} |\Psi_O\rangle \\ (\hat{o})_o |\Psi_O\rangle &= 0 \end{aligned} \quad (20)$$

Although such a decomposition is not unique as just described, if only the action upon the reference state  $|\Psi_O\rangle$  is relevant for a specific purpose, then any convenient such partitioning will suffice. If  $\hat{o}$  is already written as a linear combination of normal-ordered strings, then the straightforward choice of  $(\hat{o})_o$  consists of summing all such terms whose string contains at least one operator that is not an excitation. The corresponding choice of  $(\hat{o})_x$  then consists of the remaining terms, *i.e.*, linear combination of strings of excitations only, and perhaps a constant. For convenience, we also allow commutator brackets to be subscripted as  $[,]_x$ , indicating that only the constant and excitation part of the normal-ordered form of the result are retained.

The central task in a given CC iteration may now be framed in terms of resolving the operator  $\hat{\Omega} = (e^{-\hat{T}} \hat{\mathcal{H}} e^{\hat{T}})_x$ . The constant part of  $\hat{\Omega}$  is the CC pseudo-energy, which can also be written as  $\langle \Psi^O | \Omega \rangle$ , with  $|\Omega\rangle = \hat{\Omega} |\Psi_O\rangle$ . Projections  $\langle \Psi^I | \Omega \rangle$  onto excited complement configurations of the form  $\langle \Psi^I | = \langle \Psi^O | \hat{d}_{o_{m_1}}^{u_{m_1}} \cdots \hat{d}_{o_{m_M}}^{u_{m_M}}$  are used to determine the iterative updates to the associated amplitudes  $t_M^{u_{m_1} \cdots u_{m_M}}$ , in conjunction with multiplication by index-dependent scalars (algorithm-dependent preconditioners). This involves computing excitations in  $\hat{\Omega}$  up to the user-specified Ansatz order.

We will now proceed to similarity transform the individual operator strings found in the

Hamiltonian. For interaction terms up to the maximum possible number of single-fragment operators for electronic systems (four) we have

$$\begin{aligned}
(e^{-\hat{T}} \hat{g}_m e^{\hat{T}})_x &= (\bar{g}_m)_x \\
(e^{-\hat{T}} \hat{g}_{m_1} \hat{g}_{m_2} e^{\hat{T}})_x &= (\bar{g}_{m_1} \bar{g}_{m_2})_x \\
&= (((\bar{g}_{m_1})_x + (\bar{g}_{m_1})_o)(\bar{g}_{m_2})_x)_x \\
&= ((\bar{g}_{m_1})_x (\bar{g}_{m_2})_x + (\bar{g}_{m_1})_o (\bar{g}_{m_2})_x)_x \\
&= (\bar{g}_{m_1})_x (\bar{g}_{m_2})_x + [(\bar{g}_{m_1})_o, (\bar{g}_{m_2})_x]_x \\
(e^{-\hat{T}} \hat{g}_{m_1} \hat{g}_{m_2} \hat{g}_{m_3} e^{\hat{T}})_x &= (\bar{g}_{m_1})_x (\bar{g}_{m_2})_x (\bar{g}_{m_3})_x + (\bar{g}_{m_1})_x [(\bar{g}_{m_2})_o, (\bar{g}_{m_3})_x]_x \\
&\quad + [(\bar{g}_{m_1})_o, (\bar{g}_{m_2})_x (\bar{g}_{m_3})_x]_x + [(\bar{g}_{m_1})_o, [(\bar{g}_{m_2})_o, (\bar{g}_{m_3})_x]_x]_x \\
(e^{-\hat{T}} \hat{g}_{m_1} \hat{g}_{m_2} \hat{g}_{m_3} \hat{g}_{m_4} e^{\hat{T}})_x &= (\bar{g}_{m_1})_x (\bar{g}_{m_2})_x (\bar{g}_{m_3})_x (\bar{g}_{m_4})_x + (\bar{g}_{m_1})_x (\bar{g}_{m_2})_x [(\bar{g}_{m_3})_o, (\bar{g}_{m_4})_x]_x \\
&\quad + (\bar{g}_{m_1})_x [(\bar{g}_{m_2})_o, (\bar{g}_{m_3})_x (\bar{g}_{m_4})_x]_x + (\bar{g}_{m_1})_x [(\bar{g}_{m_2})_o, [(\bar{g}_{m_3})_o, (\bar{g}_{m_4})_x]_x]_x \\
&\quad + [(\bar{g}_{m_1})_o, (\bar{g}_{m_2})_x (\bar{g}_{m_3})_x (\bar{g}_{m_4})_x]_x + [(\bar{g}_{m_1})_o, (\bar{g}_{m_2})_x [(\bar{g}_{m_3})_o, (\bar{g}_{m_4})_x]_x]_x \\
&\quad + [(\bar{g}_{m_1})_o, [(\bar{g}_{m_2})_o, (\bar{g}_{m_3})_x (\bar{g}_{m_4})_x]_x]_x + [(\bar{g}_{m_1})_o, [(\bar{g}_{m_2})_o, [(\bar{g}_{m_3})_o, (\bar{g}_{m_4})_x]_x]_x]_x
\end{aligned} \tag{21}$$

The results for trimers and tetramers are obtained by recurring the procedure shown for the dimer term. The logic in resolving the dimer term is as follows: after inserting  $1 = e^{\hat{T}} e^{-\hat{T}}$  between the two single-fragment operators, each of the resulting normal-ordered transformed operators is divided into the parts that do and do not destroy the reference. Only the  $(\cdot)_x$  part of the right-most operator needs to be retained, since inclusion of the  $(\cdot)_o$  part simply results in additional normal-ordered terms that all destroy the reference, and therefore do not survive the outermost retention of only non-reference-destroying terms. Likewise, inclusion of the second term of the commutator shown does not change anything, since it consists only of reference-destroying terms that are not retained. However, expressing the result in terms of this commutator will prove valuable; since the second argument to the commutator consists only of constants and excitation strings, it is clear that fragment rank is hereby reduced.

To proceed, we now require explicit forms of the transformed single-fragment operators. Inserting the results of eq. (10) into eqs. (11) and (19), and again using an overbar to denote

a similarity transformed operator, we have

$$\begin{aligned}
\bar{e}_{u_m}^{o_m} &= \hat{e}_{u_m}^{o_m} \\
\bar{f}_{o_m}^{o_m} &= \hat{f}_{o_m}^{o_m} + \sum_{w_m} \hat{T}^{w_m} \hat{e}_{w_m}^{o_m} \\
\bar{f}_{u_m}^{v_m} &= \hat{f}_{u_m}^{v_m} + \hat{T}^{v_m} \hat{e}_{u_m}^{o_m} \\
\bar{d}_{o_m}^{u_m} &= \hat{d}_{o_m}^{u_m} - (\hat{T}^{u_m} \hat{f}_{o_m}^{o_m} + \sum_{w_m} \hat{T}^{w_m} \hat{f}_{w_m}^{u_m}) + \hat{T}^{u_m} \left(1 - \sum_{w_m} \hat{T}^{w_m} \hat{e}_{w_m}^{o_m}\right)
\end{aligned} \tag{22}$$

each of which is easily divided into an  $()_x$  part (the last or only term) and other  $()_o$  terms.

We will now confine our attention here to the dimer Hamiltonian terms that were implemented for this work. The procedure for higher-fragment-order terms is a straightforward repetition of this procedure, albeit, increasingly tedious. If we now arbitrarily decide that normal ordering also involves having any de-excitation operators to the far right and having any virtual-rearrangement flat operators ( $\hat{f}_{u_m}^{v_m}$ ) to the right of any reference-hole-check flat operators ( $\hat{f}_{o_m}^{o_m}$ ), then we have 10 classes of dimer terms in the normal-ordered Hamiltonian:  $\hat{e}_{u_{m1}}^{o_{m1}} \hat{e}_{u_{m2}}^{o_{m2}}$ ,  $\hat{e}_{u_{m1}}^{o_{m1}} \hat{f}_{o_{m2}}^{o_{m2}}$ ,  $\hat{e}_{u_{m1}}^{o_{m1}} \hat{f}_{u_{m2}}^{v_{m2}}$ ,  $\hat{e}_{u_{m1}}^{o_{m1}} \hat{d}_{o_{m2}}^{u_{m2}}$ ,  $\hat{f}_{o_{m1}}^{o_{m1}} \hat{f}_{o_{m2}}^{o_{m2}}$ ,  $\hat{f}_{o_{m1}}^{o_{m1}} \hat{f}_{u_{m2}}^{v_{m2}}$ ,  $\hat{f}_{o_{m1}}^{o_{m1}} \hat{d}_{o_{m2}}^{u_{m2}}$ ,  $\hat{f}_{u_{m1}}^{v_{m1}} \hat{f}_{u_{m2}}^{v_{m2}}$ ,  $\hat{f}_{u_{m1}}^{v_{m1}} \hat{d}_{o_{m2}}^{u_{m2}}$ ,  $\hat{d}_{o_{m1}}^{u_{m1}} \hat{d}_{o_{m2}}^{u_{m2}}$ .

The non-zero commutators of eq. (21) that are then needed are

$$\begin{aligned}
[(\bar{f}_{o_{m_1}}^{o_{m_1}})_o, (\bar{f}_{o_{m_2}}^{o_{m_2}})_x]_x &= \sum_{w_{m_1}, w_{m_2}} \hat{T}^{w_{m_1}, w_{m_2}} \hat{e}_{w_{m_1}}^{o_{m_1}} \hat{e}_{w_{m_2}}^{o_{m_2}} \\
[(\bar{f}_{o_{m_1}}^{o_{m_1}})_o, (\bar{f}_{u_{m_2}}^{v_{m_2}})_x]_x &= \sum_{w_{m_1}} \hat{T}^{w_{m_1}, v_{m_2}} \hat{e}_{w_{m_1}}^{o_{m_1}} \hat{e}_{u_{m_2}}^{o_{m_2}} \\
[(\bar{f}_{o_{m_1}}^{o_{m_1}})_o, (\bar{d}_{o_{m_2}}^{u_{m_2}})_x]_x &= \sum_{w_{m_1}} \hat{T}^{w_{m_1} u_{m_2}} \hat{e}_{w_{m_1}}^{o_{m_1}} - \sum_{w_{m_1}, w_{m_2}} \left( \hat{T}^{w_{m_1} u_{m_2}} \hat{T}^{w_{m_2}} + \hat{T}^{w_{m_1} w_{m_2}} \hat{T}^{u_{m_2}} \right) \hat{e}_{w_{m_1}}^{o_{m_1}} \hat{e}_{w_{m_2}}^{o_{m_2}} \\
[(\bar{f}_{u_{m_1}}^{v_{m_1}})_o, (\bar{f}_{u_{m_2}}^{v_{m_2}})_x]_x &= \hat{T}^{v_{m_1} v_{m_2}} \hat{e}_{u_{m_1}}^{o_{m_1}} \hat{e}_{u_{m_2}}^{o_{m_2}} \\
[(\bar{f}_{u_{m_1}}^{v_{m_1}})_o, (\bar{d}_{o_{m_2}}^{u_{m_2}})_x]_x &= \hat{T}^{v_{m_1} u_{m_2}} \hat{e}_{u_{m_1}}^{o_{m_1}} - \sum_{w_{m_2}} \left( \hat{T}^{v_{m_1} u_{m_2}} \hat{T}^{w_{m_2}} + \hat{T}^{v_{m_1} w_{m_2}} \hat{T}^{u_{m_2}} \right) \hat{e}_{u_{m_1}}^{o_{m_1}} \hat{e}_{w_{m_2}}^{o_{m_2}} \\
[(\bar{d}_{o_{m_1}}^{u_{m_1}})_o, (\bar{d}_{o_{m_2}}^{u_{m_2}})_x]_x &= \hat{T}^{u_{m_1} u_{m_2}} \\
&\quad - \sum_{w_{m_1}} \left( \hat{T}^{u_{m_1}} \hat{T}^{w_{m_1} u_{m_2}} + \hat{T}^{w_{m_1}} \hat{T}^{u_{m_1} u_{m_2}} \right) \hat{e}_{w_{m_1}}^{o_{m_1}} \\
&\quad - \sum_{w_{m_2}} \left( \hat{T}^{u_{m_1} u_{m_2}} \hat{T}^{w_{m_2}} + \hat{T}^{u_{m_1} w_{m_2}} \hat{T}^{u_{m_2}} \right) \hat{e}_{w_{m_2}}^{o_{m_2}} \\
&\quad + \sum_{w_{m_1}, w_{m_2}} \left( \hat{T}^{u_{m_1} u_{m_2}} \hat{T}^{w_{m_1} w_{m_2}} + \hat{T}^{u_{m_1} w_{m_2}} \hat{T}^{w_{m_1} u_{m_2}} \right. \\
&\quad \quad \left. + \hat{T}^{u_{m_1}} \hat{T}^{w_{m_1} u_{m_2}} \hat{T}^{w_{m_2}} + \hat{T}^{w_{m_1}} \hat{T}^{u_{m_1} u_{m_2}} \hat{T}^{w_{m_2}} \right. \\
&\quad \quad \left. + \hat{T}^{u_{m_1}} \hat{T}^{w_{m_1} w_{m_2}} \hat{T}^{u_{m_2}} + \hat{T}^{w_{m_1}} \hat{T}^{u_{m_1} w_{m_2}} \hat{T}^{u_{m_2}} \right) \hat{e}_{w_{m_1}}^{o_{m_1}} \hat{e}_{w_{m_2}}^{o_{m_2}}
\end{aligned} \tag{23}$$

which make use of the fact that  $m_1 \neq m_2$ .

We now further confine our attention to the X2-CCSD model, for which we also have

$$\begin{aligned}
\hat{T}^{w_m} &= t_1^{w_m} + \sum_{m', w_{m'}} t_2^{w_m w_{m'}} \hat{e}_{w_{m'}}^{o_{m'}} \\
\hat{T}^{w_{m_1} w_{m_2}} &= t_2^{w_{m_1} w_{m_2}}
\end{aligned} \tag{24}$$

In order to then resolve  $\hat{\Omega}$  for this model, eqs. (23) and (24) are inserted into eq. (21) for each class of dimer terms, and the resulting similarity transformed operators are linearly combined according to the matrix elements of the normal-ordered Hamiltonian, such that if we decompose  $\hat{\Omega}$  as

$$\hat{\Omega} = \Omega_0 + \sum_{m, u_m} \Omega_1^{u_m} \hat{e}_{u_m}^{o_m} + \frac{1}{2} \sum_{m_1, u_{m_1}} \sum_{m_2, u_{m_2}} \Omega_2^{u_{m_1} u_{m_2}} \hat{e}_{u_{m_1}}^{o_{m_1}} \hat{e}_{u_{m_2}}^{o_{m_2}} + \dots \tag{25}$$

the coefficients for up to dimer terms can be written as

$$\begin{aligned}
\Omega_0 &= \mathcal{H}_x^o t_1^{\dot{x}} + \mathcal{H}_{\dot{x}\dot{x}'}^o t_{\text{II}}^{\dot{x}\dot{x}'} \\
\Omega_1^{u_m} &= \mathcal{H}_{o_m}^{u_m} + \mathcal{H}_{o_m}^{o_m} t_1^{u_m} + \mathcal{H}_{\dot{x}_m}^{u_m} t_1^{\dot{x}_m} + \mathcal{H}_{\dot{x}}^{o_m} t_2^{\dot{x}_m} - \mathcal{H}_{\dot{x}_m}^{o_m} t_1^{\dot{x}_m} t_1^{u_m} + \mathcal{H}_{o_m}^{u_m o} t_1^{\dot{x}} + \mathcal{H}_{o_m}^{o_m o} t_{\text{II}}^{\dot{x}_m} + \mathcal{H}_{\dot{x}_m}^{u_m o} t_{\text{II}}^{\dot{x}_m} \\
&\quad + 2\mathcal{H}_{\dot{x}\dot{x}'}^o t_1^{\dot{x}'} t_2^{\dot{x}_m} - 2\mathcal{H}_{\dot{x}\dot{x}_m}^{o o_m} t_1^{\dot{x}_m} t_2^{\dot{x}_m} - 2\mathcal{H}_{\dot{x}_m \dot{x}}^{o_m o} t_{\text{II}}^{\dot{x}_m} t_1^{u_m} \\
\Omega_2^{u_{m_1} u_{m_2}} &= \mathcal{H}_{o_{m_1}}^{o_{m_1}} t_2^{u_{m_1} u_{m_2}} + \mathcal{H}_{\dot{x}_{m_1}}^{u_{m_1}} t_2^{\dot{x}_{m_1} u_{m_2}} - \mathcal{H}_{\dot{x}_{m_1}}^{o_{m_1}} t_1^{\dot{x}_{m_1}} t_2^{u_{m_1} u_{m_2}} - \mathcal{H}_{\dot{x}_{m_2}}^{o_{m_2}} t_2^{\dot{x}_{m_2} u_{m_1}} t_1^{u_{m_2}} \\
&\quad + \mathcal{H}_{o_{m_1} o_{m_2}}^{u_{m_1} u_{m_2}} + \mathcal{H}_{o_{m_1} o_{m_2}}^{u_{m_1} o_{m_2}} t_1^{u_{m_2}} + \mathcal{H}_{o_{m_1} \dot{x}_{m_2}}^{u_{m_1} u_{m_2}} t_1^{\dot{x}_{m_2}} + \mathcal{H}_{o_{m_1} \dot{x}}^{u_{m_1} o} t_2^{\dot{x} u_{m_2}} - \mathcal{H}_{o_{m_1} \dot{x}_{m_2}}^{u_{m_1} o_{m_2}} t_1^{\dot{x}_{m_2}} t_1^{u_{m_2}} \\
&\quad + \mathcal{H}_{o_{m_1} o_{m_2}}^{o_{m_1} o_{m_2}} t_{\text{II}}^{u_{m_1} u_{m_2}} + \mathcal{H}_{o_{m_2} \dot{x}_{m_1}}^{o_{m_2} u_{m_1}} t_{\text{II}}^{\dot{x}_{m_1} u_{m_2}} + \mathcal{H}_{o_{m_2} \dot{x}}^{o_{m_2} o} t_2^{\dot{x} u_{m_1}} t_1^{u_{m_2}} - \mathcal{H}_{o_{m_1} \dot{x}_{m_2}}^{o_{m_1} o_{m_2}} t_2^{\dot{x}_{m_2} u_{m_1}} t_1^{u_{m_2}} \\
&\quad + \mathcal{H}_{o_{m_1} \dot{x}}^{o_{m_1} o} t_1^{\dot{x} u_{m_1} u_{m_2}} - \mathcal{H}_{o_{m_1} \dot{x}_{m_2}}^{o_{m_1} o_{m_2}} t_1^{\dot{x}_{m_2} u_{m_1}} t_{\text{II}}^{u_{m_2}} + \mathcal{H}_{\dot{x}_{m_1} \dot{x}_{m_2}}^{u_{m_1} u_{m_2}} t_{\text{II}}^{\dot{x}_{m_1} \dot{x}_{m_2}} + \mathcal{H}_{\dot{x}_{m_1} \dot{x}}^{u_{m_1} o} t_1^{\dot{x} \dot{x}_{m_1} u_{m_2}} \\
&\quad + \mathcal{H}_{\dot{x}_{m_1} \dot{x}}^{u_{m_1} o} t_1^{\dot{x}_{m_1} \dot{x}_{m_2} u_{m_2}} - \mathcal{H}_{\dot{x}_{m_1} \dot{x}_{m_2}}^{u_{m_1} o_{m_2}} t_1^{\dot{x}_{m_2} \dot{x}_{m_1} u_{m_2}} - \mathcal{H}_{\dot{x}_{m_1} \dot{x}_{m_2}}^{u_{m_1} o_{m_2}} t_{\text{II}}^{\dot{x}_{m_1} \dot{x}_{m_2} u_{m_1}} t_1^{u_{m_2}} + \mathcal{H}_{\dot{x}\dot{x}'}^{o o} t_2^{\dot{x}' u_{m_1}} t_1^{\dot{x}_{m_2}} \\
&\quad - 2\mathcal{H}_{\dot{x}\dot{x}_m}^{o o_m} t_1^{\dot{x}_{m_2}} t_2^{u_{m_1}} - 2\mathcal{H}_{\dot{x}_{m_2} \dot{x}}^{o_{m_2} o} t_1^{\dot{x}} t_2^{\dot{x}_{m_2} u_{m_1}} t_1^{u_{m_2}} + 2\mathcal{H}_{\dot{x}_{m_2} \dot{x}_{m_1}}^{o_{m_2} o_{m_1}} t_1^{\dot{x}_{m_1}} t_2^{\dot{x}_{m_2} u_{m_1}} t_1^{u_{m_2}} \\
&\quad - 2\mathcal{H}_{\dot{x}\dot{x}_{m_2}}^{o o_m} t_2^{\dot{x}_{m_2}} t_1^{u_{m_1}} + \mathcal{H}_{\dot{x}_{m_1} \dot{x}_{m_2}}^{o_{m_1} o_{m_2}} t_2^{\dot{x}_{m_2} u_{m_1}} t_1^{u_{m_1}} \\
&\quad - 2\mathcal{H}_{\dot{x}_{m_1} \dot{x}}^{o_{m_1} o} t_{\text{II}}^{\dot{x}_{m_1} \dot{x}} t_2^{u_{m_1} u_{m_2}} + \mathcal{H}_{\dot{x}_{m_1} \dot{x}_{m_2}}^{o_{m_1} o_{m_2}} t_{\text{II}}^{\dot{x}_{m_1} \dot{x}_{m_2}} t_1^{u_{m_1} u_{m_2}}
\end{aligned} \tag{26}$$

where we have defined

$$t_{\text{II}}^{u_{m_1} u_{m_2}} = t_2^{u_{m_1} u_{m_2}} + t_1^{u_{m_1}} t_1^{u_{m_2}} \tag{27}$$

The contraction notation here is essentially the Einstein summation convention, except that contracted indices are explicitly indicated by the placement of a dot above them (preventing confusion of summations and diagonal elements). If a contracted index is not subscripted by the label of a fragment, summation over all fragments is additionally implied. The matrix elements with which the amplitudes are contracted are from the normal-ordered Hamiltonian,

such that

$$\begin{aligned}
\mathcal{H}_0 &= \sum_{m'} H_{o_m}^{o_{m'}} + \frac{1}{2} \sum_{m', m''} H_{o_m o_{m''}}^{o_{m'} o_{m''}} \\
\mathcal{H}_{o_m}^{u_m} &= H_{o_m}^{u_m} + \sum_{m'} H_{o_m o_{m'}}^{u_m o_{m'}} \\
\mathcal{H}_{o_m}^{o_m} &= -\left( H_{o_m}^{o_m} + \sum_{m'} H_{o_m o_{m'}}^{o_m o_{m'}} \right) \\
\mathcal{H}_{v_m}^{u_m} &= H_{v_m}^{u_m} + \sum_{m'} H_{v_m o_{m'}}^{u_m o_{m'}} \\
\mathcal{H}_{u_m}^{o_m} &= H_{u_m}^{o_m} + \sum_{m'} H_{u_m o_{m'}}^{o_m o_{m'}} \\
\mathcal{H}_{o_{m_1} o_{m_2}}^{u_{m_1} u_{m_2}} &= \frac{1}{2} H_{o_{m_1} o_{m_2}}^{u_{m_1} u_{m_2}} \\
\mathcal{H}_{o_{m_1} o_{m_2}}^{u_{m_1} o_{m_2}} &= -H_{o_{m_1} o_{m_2}}^{u_{m_1} o_{m_2}} \\
\mathcal{H}_{o_{m_1} v_{m_2}}^{u_{m_1} u_{m_2}} &= H_{o_{m_1} v_{m_2}}^{u_{m_1} u_{m_2}} \\
\mathcal{H}_{o_{m_1} u_{m_2}}^{u_{m_1} o_{m_2}} &= H_{o_{m_1} u_{m_2}}^{u_{m_1} o_{m_2}} \\
\mathcal{H}_{o_{m_1} o_{m_2}}^{o_{m_1} o_{m_2}} &= \frac{1}{2} H_{o_{m_1} o_{m_2}}^{o_{m_1} o_{m_2}} \\
\mathcal{H}_{o_{m_1} v_{m_2}}^{o_{m_1} u_{m_2}} &= -H_{o_{m_1} v_{m_2}}^{o_{m_1} u_{m_2}} \\
\mathcal{H}_{o_{m_1} u_{m_2}}^{o_{m_1} o_{m_2}} &= -H_{o_{m_1} u_{m_2}}^{o_{m_1} o_{m_2}} \\
\mathcal{H}_{v_{m_1} v_{m_2}}^{u_{m_1} u_{m_2}} &= \frac{1}{2} H_{v_{m_1} v_{m_2}}^{u_{m_1} u_{m_2}} \\
\mathcal{H}_{v_{m_1} u_{m_2}}^{u_{m_1} o_{m_2}} &= H_{v_{m_1} u_{m_2}}^{u_{m_1} o_{m_2}} \\
\mathcal{H}_{u_{m_1} u_{m_2}}^{o_{m_1} o_{m_2}} &= \frac{1}{2} H_{u_{m_1} u_{m_2}}^{o_{m_1} o_{m_2}}
\end{aligned} \tag{28}$$

where the raw matrix elements on the right-hand sides of eq. (28) are those from the Hamiltonian expansion in the main text of the article, except that the main article only defines them for  $m_1 < m_2$ . As with the amplitudes we may simply assert that the otherwise undefined elements are identical to that in which the upper and lower indices are simultaneously permuted, with zero resulting for  $m_1 = m_2$ . In finalizing the above expressions we have often made use of such permutational symmetries to better organize the indices. It is worth noting that, as its elements are written, the tensor  $\Omega_2$  is not symmetric with respect to permutation of indices, as this would require the inclusion of additional terms that constitute substantially similar computations. This tensor can simply be symmetrized without resulting in any change to  $\hat{\Omega}$  in eq. (25); this can be done efficiently in a *post hoc* step. In practice, this is required, in order

that the resulting update to  $\mathbf{t}_2$  preserves the asserted permutational symmetry, on which the validity of the foregoing derivation rests.

Two different implementations of the amplitude equations were used, stemming from two different points in the above derivation. A more abstract implementation is based on direct representation of the operators in eqs. (21) – (23) and a loop over all terms in the Hamiltonian, with some minor adjustments to avoid implicit loops of spuriously high scaling. The advantage of this approach is that the code contains relatively few lines, which are easily validated by eye against the original equations. This code is quite slow, however, relative to the direct implementation of the explicit tensor contractions written in eq. (26). A much faster implementation is based on eq. (26), with some factorizations to decrease redundancy. Aside from the definition of the tensor intermediate  $\mathbf{t}_{\text{II}}$ , no such factorizations are shown above. We deem these aspects, along with a discussion of optimal partially contracted intermediates, to be details best discussed in a future publication on algorithm optimization (but the individual terms are written here with the contractions in the most efficient order, from left to right). As currently implemented, the algorithm requires a scratch space for intermediates that scales linearly with the system size.

Mutual numerical consistency within a validation chain of independent programs was used to verify that the amplitude equations were implemented correctly. First, since it would be arduous to adapt the CC codes of established quantum chemistry packages to perform excitonic calculations via the previously mentioned fermionic mapping, we implemented the well-known conventional CCSD equations,<sup>37</sup> in an in-house program. The first link of the validation chain was to check the in-house conventional CCSD code (operating with the usual one- and two-electron integrals) against established packages for small electronic systems (*e.g.*, frozen core Be dimer). These checks agreed to all digits for which the package software was reliable (*i.e.*, accounting for thresholds). This served to validate not only our implementation of the conventional CC amplitude equations, but also the quasi-Newton/DIIS nonlinear optimization algorithm in which they are embedded. All in-house codes use the same CC iteration machinery, aside from the amplitude equations (the internal structure of  $\hat{\mathcal{H}}$  and  $\hat{T}$  are hidden from the nonlinear optimizer). Our conventional CC code could then be fed the matrix elements for small oscillator-model fragment Hamiltonians, using the stated fermionic mapping. For these systems, mutual consistency of this fermionically mapped code with the aforementioned

abstract implementation of the X2-CCSD amplitude equations served to validate both. The Be-fragment Hamiltonians for small numbers of fragments were then formatted for both the abstract and the explicit implementations, allowing us to thereby validate the more efficient implementation. For all of the comparisons between our three completely independent implementations of the X2-CCSD amplitude equations (fermionically mapped, and two directly excitonic implementations), test results agreed to within machine precision.

## References

- (1) K. Kitaura, E. Ikeo, T. Asada, T. Nakano, and M. Uebayasi, *Chem. Phys. Lett.* **313**, 701 (1999).
- (2) S. Hirata, M. Valiev, M. Dupuis, S. S. Xantheas, S. Sugiki, and H. Sekino, *Mol. Phys.* **103**, 2255 (2005).
- (3) D. G. Fedorov and K. Kitaura, *J. Phys. Chem.* **111**, 6904 (2007).
- (4) M. Kamiya, S. Hirata, and M. Valiev, *J. Chem. Phys.* **128**, 074103 (2008).
- (5) L. D. Jacobson and J. M. Herbert, *J. Chem. Phys.* **134**, 094118 (2011).
- (6) P. J. Bygrave, N. L. Allan, and F. R. Manby, *J. Chem. Phys.* **137**, 164102 (2012).
- (7) F. R. Manby, M. Stella, J. D. Goodpaster, and T. F. Miller, III, *J. Chem. Theory Comput.* **8**, 2564 (2012).
- (8) I. W. Bulik, W. Chen, and G. E. Scuseria, *J. Chem. Phys.* **141**, 054113 (2014).
- (9) T. Dresselhaus and J. Neugebauer, *Theor. Chem. Acc.* **134**, 97 (2015).
- (10) B. Jeziorski, R. Moszynski, and K. Szalewicz, *Chem. Rev.* **94**, 1887 (1994).
- (11) J. N. Byrd, N. Jindal, R. W. Molt, Jr., R. J. Bartlett, B. A. Sanders, and V. F. Lotrich, *Mol. Phys.* **113**, 3459 (2015).
- (12) S. J. Nolan, P. J. Bygrave, N. L. Allan, and F. R. Manby, *J. Phys.: Condens. Matter* **22**, 074201 (2010).
- (13) C. Müller, D. Usvyat, and H. Stoll, *Phys. Rev. B* **83**, 245136 (2011).
- (14) G. J. O. Beran, *Chem. Rev.* **116**, 5567 (2016).
- (15) M. S. Gordon, D. G. Fedorov, S. R. Pruitt, and L. V. Slipchenko, *Chem. Rev.* **112**, 632 (2011).
- (16) R. M. Richard and J. M. Herbert, *J. Chem. Phys.* **137**, 064113 (2012).
- (17) M. A. Collins and R. P. A. Bettens, *Chem. Rev.* **115**, 5607 (2015).
- (18) K. Raghavachari and A. Saha, *Chem. Rev.* **115**, 5643 (2015).
- (19) O. Christiansen, *J. Chem. Phys.* **120**, 2140 (2004).
- (20) P. Seidler and O. Christiansen, in *Challenges and Advances in Computational Chemistry and Physics*, edited by P. Cársky, J. Paldus, and J. Pittner (Springer Netherlands, Dordrecht, 2010), Vol. 11, p. 491.
- (21) J. A. Faucheaux and S. Hirata, *J. Chem. Phys.* **143**, 134105 (2015).
- (22) J. Frenkel, *Phys. Rev.* **37**, 17 (1931).

(23) A. S. Davydov, *Theory of Molecular Excitons* (Plenum, New York, 1971).

(24) V. May and O. Kühn, *Charge and Energy Transfer Dynamics in Molecular Systems* (Wiley, Weinheim, Germany, 2011).

(25) A. Sisto, D. R. Glowacki, and T. J. Martinez, *Acc. Chem. Res.* **47**, 2857 (2014).

(26) A. F. Morrison and J. M. Herbert, *J. Phys. Chem. Lett.* **6**, 4390 (2015).

(27) A. Stone, *The Theory of Intermolecular Forces* (Oxford University Press, Oxford, 2013).

(28) T. Korona, *J. Chem. Theory Comput.* **5**, 2663 (2009).

(29) R. Podeszwa and K. Szalewicz, *J. Chem. Phys.* **126**, 194101 (2007).

(30) J. Cui, H. Liu, and K. D. Jordan, *J. Phys. Chem. B* **110**, 18872 (2006).

(31) K. U. Lao, K.-Y. Liu, R. M. Richard, and J. M. Herbert, *J. Chem. Phys.* **144**, 164105 (2016).

(32) K. E. Riley, M. Pitoňák, P. Jurečka, and P. Hobza, *Chem. Rev.* **110**, 5023 (2010).

(33) A. Ambrosetti, N. Ferri, R. A. DiStasio, Jr., and A. Tkatchenko, *Science* **351**, 1171 (2016).

(34) S. R. White, *Phys. Rev. Lett.* **69**, 2863 (1992).

(35) G. K.-L. Chan and S. Sharma, *Annu. Rev. Phys. Chem.* **62**, 465 (2011).

(36) E. D. Hedegård, S. Knecht, J. S. Kielberg, H. J. A. Jensen, and M. Reiher, *J. Chem. Phys.* **142**, 224108 (2015).

(37) T. Helgaker, P. Jorgensen, and J. Olsen, *Molecular Electronic-Structure Theory* (Wiley, Sussex, 2002).

(38) R. M. Parrish, L. A. Burns, D. G. A. Smith, A. C. Simmonett, A. E. DePrince, III, E. G. Hohenstein, U. Bozkaya, A. Y. Sokolov, R. Di Remigio, R. M. Richard, J. F. Gonthier, A. M. James, H. R. McAlexander, A. Kumar, M. Saitow, X. Wang, B. P. Pritchard, P. Verma, H. F. Schaefer, III, K. Patkowski, R. A. King, E. F. Valeev, F. A. Evangelista, J. M. Turney, T. D. Crawford, and C. D. Sherrill, *J. Chem. Theory Comput.* **13**, 3185 (2017).

(39) R. P. Muller, PyQuante: Python Quantum Chemistry, <http://pyquante.sourceforge.net/>, 2014, [Accessed 25-October-2016].

(40) R. H. Ewing and A. M. Mellor, *J. Chem. Phys.* **53**, 2983 (1970).

(41) M. R. A. Blomberg and P. E. M. Siegbahn, *Int. J. Quantum Chem.* **14**, 583 (1978).

(42) V. E. Bondybey and J. H. English, *J. Chem. Phys.* **80**, 568 (1984).

(43) K. Kowalski, S. Hirata, M. Włoch, P. Piecuch, and T. L. Windus, *J. Chem. Phys.* **123**, 074319 (2005).

(44) J. M. Merritt, V. E. Bondybey, and M. C. Heaven, *Science* **324**, 1548 (2009).

(45) M. El Khatib, G. L. Bendazzoli, S. Evangelisti, W. Helal, T. Leininger, L. Tenti, and C. Angeli, *J. Phys. Chem. A* **118**, 6664 (2014).

(46) S. Sharma, T. Yanai, G. H. Booth, C. J. Umrigar, and G. K.-L. Chan, *J. Chem. Phys.* **140**, 104112 (2014).

(47) V. V. Meshkov, A. V. Stolyarov, M. C. Heaven, C. Haugen, and R. J. LeRoy, *J. Chem. Phys.* **140**, 064315 (2014).

(48) A. D. Dutoi, Y. Jung, and M. Head-Gordon, *J. Phys. Chem. A* **108**, 10270 (2004).

(49) R. Z. Khaliullin, A. T. Bell, and M. Head-Gordon, *Chem. Eur. J.* **15**, 851 (2009).

(50) C. C. Paige, *IMA J. Appl. Math.* **10**, 373 (1972).

(51) A. D. Dutoi, L. S. Cederbaum, M. Wormit, J. H. Starcke, and A. Dreuw, *J. Chem. Phys.* **132**, 144302 (2010).

(52) A. Kramida and W. C. Martin, *J. Phys. Chem. Ref. Data* **26**, 1185 (1997).

(53) R. Mota, R. Parafita, A. Giuliani, M.-J. Hubin-Franksin, J. M. C. Lourenço, G. Garcia, S. V. Hoffmann, N. J. Mason, P. A. Ribeiro, M. Raposo, and P. Limão-Vieira, *Chem. Phys. Lett.* **416**, 152 (2005).

(54) B. K. Sahoo and B. P. Das, *Phys. Rev. A* **77**, 062516 (2008).

(55) W. F. Murphy, *J. Chem. Phys.* **67**, 5877 (1977).

(56) J. Yang, G. K.-L. Chan, F. R. Manby, M. Schütz, and H.-J. Werner, *J. Chem. Phys.* **136**, 144105 (2012).

(57) A. G. Taube and R. J. Bartlett, *J. Chem. Phys.* **128**, 164101 (2008).

(58) A. E. DePrince, III and C. D. Sherrill, *J. Chem. Theory Comput.* **9**, 2687 (2013).

(59) F. Neese, F. Wennmohs, and A. Hansen, *J. Chem. Phys.* **130**, 114108 (2009).

(60) C. Riplinger, B. Sandhoefer, A. Hansen, and F. Neese, *J. Chem. Phys.* **139**, 134101 (2013).

(61) D. Mukherjee, R. K. Moitra, and A. Mukhopadhyay, *Mol. Phys.* **30**, 1861 (1975).

(62) B. Jeziorski and H. J. Monkhorst, *Phys. Rev. A* **24**, 1668 (1981).

(63) J. Paldus and X. Li, *Adv. Chem. Phys.* **110**, 1 (1999).

(64) T. Kinoshita, O. Hino, and R. J. Bartlett, *J. Chem. Phys.* **123**, 074106 (2005).

(65) T. Yanai and G. K.-L. Chan, *J. Chem. Phys.* **124**, 194106 (2006).

(66) F. A. Evangelista, M. Hanauer, A. Köhn, and J. Gauss, *J. Chem. Phys.* **136**, 204108 (2012).

(67) H. Koch and P. Jørgensen, *J. Chem. Phys.* **93**, 3333 (1990).

- (68) J. F. Stanton and R. J. Bartlett, *J. Chem. Phys.* **98**, 7029 (1993).
- (69) P. M. Zimmerman, *J. Chem. Phys.* **146**, 224104 (2017).
- (70) P. Seidler and O. Christiansen, *J. Chem. Phys.* **131**, 234109 (2009).